Dynamical simulation of β Pic dust: implications for the amount of gas in the disk

Ghanjah Skånby-Mansour

Master thesis (examensarbete) at the Department of Astronomy, su

September 25, 2003

Contents

1 Introduction **2**
- 1.1 Star formation . . . 2
- 1.2 The molecular cloud . . . 2
- 1.3 The collapse of the molecular cloud cores and star formation . . . 3
- 1.4 The observations of star formation . . . 3
- 1.5 Observation of circumstellar disk . . . 4
- 1.6 The Protoplanetary disk . . . 4
  - 1.6.1 The infall stage . . . 4
  - 1.6.2 The internal dynamical evolution of the disk . . . 5

2 Vega-type stars **6**

3 β Pic **6**
- 3.1 The IR excess from the dust and sand . . . 7
- 3.2 Silicates in the gap . . . 8
- 3.3 The spatial distribution of grains from combined visible and IR modeling . . . 8
- 3.4 The properties of the grains . . . 10
- 3.5 Evidence for planetesimals . . . 10
- 3.6 Do the planets exist? . . . 11
- 3.7 The physical processes in dust of β Pic . . . 12
- 3.8 Collision: creating and destroying the dust . . . 13

4 The problem of gas mass in β Pic and the motivation of this work **14**
- 4.1 Numerical model . . . 15
- 4.2 The equation of motion . . . 16
- 4.3 The theoretical dust distribution . . . 18
- 4.4 The dust distribution . . . 18
- 4.5 The observed vertical dust distribution . . . 19
- 4.6 Models and discussion . . . 20

5 Summary and Conclusion **34**

6 Appendix **36**
- 6.1 The molecular cloud . . . 36
- 6.2 The infall stage . . . 36
- 6.3 The internal dynamical evolution of the disk . . . 37
- 6.4 The chemistry in the disk . . . 38
- 6.5 The properties of the grains . . . 40
- 6.6 References . . . 42

Abstract

β Pic is a Vega-type star, which means it emits infrared excess. Several observations were taken on β Pic disk and given two different ideas about the mass of β Pic disk. One is that β Pic disk has very large amount of molecular H(H_2): the observations done Thi et al (2001) give the mass of hydrogen M(H_2) $\approx 60 M_E$. The other idea is that β Pic disk has very little gas: the observations done by Lecavelier des Etangs et al. (2001) give the mass of hydrogen M(H_2) $\sim 10^{-4} M_E$, and the observations done by Brandeker et al.(2003, unpublished) give the mass of other gases than hydrogen M(gas) $\approx 0.02 M_E$. These observations create a gas mass problem which is the reason of this project. In order to resolve the gas problem I made a dynamical modeling of the vertical structure of the dust in β Pic disk, and compared the result with the observations. I traced the trajectories of 1000 to 10000 dust grains created by collisions of parent bodies and used Euler method to follow their motion. Since the dust interacts with gas and flattens the in time, my goal was to use the observed brightness of dust to limit the amount of gas. The vertical dust distribution is Gaussian. The gravitation, radiation pressure and gas drag forces are acting on dust. I chose the gas mass between 0.001 and 100 earth mass and made six models. The only model which approximately fits the observed vertical brightness is model 6 (the gas mass is equal to 0.2 earth mass). If we take the other molecules in account in the observations done by Lecavelier and the hydrogen mass in the observations done by Brandeker then my result are not inconsistent with their estimate. If we take other gases in account then the total mass of the gas in the observations done by Thi will be close to $\sim$ 100 earth mass, and according to model 5 (the gas mass is equal to 100 earth mass) the profile does not fit the observed vertical brightness profile. β Pic disk according to the observations done by Lecavelier et al. 2001, and Brandeker et al. (unpublished), and my simulation is a gas-poor disk.

1 Introduction

1.1 Star formation

Scientists believe that our Solar system was born in a dense molecular cloud as a result of the gravitational collapse. We will consider those ideas briefly.

1.2 The molecular cloud

Our galaxy or Milky Way have a huge number of cold, dense molecular cloud. Their size at the core can vary between $\sim 10^5 - 10^6 M_\odot$ in a large system to $\sim 1 M_\odot$ in smaller system.
The cores of small system are observed at radio wavelength in molecular line transitions as example NH_3,HCN,CS or H_2CO.

The temperature of the molecular cloud is in interval l $\sim 10 - 30K$, and the density of $\sim 10^3$molecular/cm^3. The density of large cores is 10-100 bigger than for the small cores. The most abundant in the molecular cloud is Hydrogen(H_2), followed by Helium(He).
we can find also many other elements (molecules) such as CO, CN, CS, SiO, OH, H_2O HCN, SO_2, H_2S, NH_3 and N_2CO. Heavy molecules make up a small percentage of the molecular cloud mass.
The stable molecular cloud has to have a balance between internal pressure and gravity forces.

If the pressure is larger than the gravity the cloud will expand and if the opposite is true the cloud will collapse.
If the molecular cloud is in an equilibrium state , the gravitational potential energy, E_G, is equal to the negative twice the kinetic energy E_k. E_k here is the thermal energy of the gas, unless the cloud is highly turbulent or rapidly rotating.

1.3 The collapse of the molecular cloud cores and star formation

The cloud collapses on a free-fall time-scale,

$$t_{eff} = \left(\frac{3\pi}{32G\rho}\right)^{1/2} \tag{1}$$

if the ratio of the pressure to gravity is very small. The rotation and the large density make the cloud fragment. If the centrifugal force is in balance with the gravitational force, the rotation would be the dominant effect on the cloud. This rapid rotation may cause the cloud to fragment in sub-clouds, each with own angular momentum. The sub-clouds in turn collapse into stars and form binary or multiple systems. If the cloud or more correctly the clump has little angular momentum only a single star forms. The cloud or clump has more angular momentum in the beginning than the formed star have. This gives an expectation that the star have a flat disk surrounding it, and the star has to have most of the total mass. As an example, our Solar System has 99.8 % of the mass in the Sun , and $\approx$ 98% of the angular momentum in the planetary orbits.

The consequence of converting the gravitational potential energy into kinetic energy in the dense core, is rise of the temperature. The thermal energy will radiate away if the cloud is transparent at infrared wavelengths. This will keep the cloud cold. But when the density increase, the cloud will be opaque, which stops the escape of the thermal energy. Here the gravitational energy heats the protostar at the center, which creates an internal pressure. This continues until the hydrostatic equilibrium is reached. When the temperature in the center of protostar reaches $\sim 10^6$K, the nuclear reactions take place.

The dust in the outer parts of the cloud makes the protostar invisible to us. The dust stay cold in the early gravitational phases (30K). Here the dust emits infrared radiation, which has the distribution peak at $\sim 100\mu m$. In the inner protostar the dust gets very high temperature that it is observed at shorter infrared wavelength.

1.4 The observations of star formation

A young star, less than 10^7years old continues to contract during its journey toward the main-sequence. It is then called a pre-main sequence star (an example of those are T Tauri stars). T Tauri stars have dense gas and dust. Their luminosity varies with timescales of few hours. Their spectral energy distributions are broader than the spectra of the blackbody. The energy spectrum is dominated by the emission line and has feature of existing strong stellar winds.

T Tauri stars have large sunspots, which allow us to measure their rotation periods. T Tauri stars emit X-rays, more than the older stars of equal mass. The early phases of star

formation and evolution can be very violent. The bipolar outflows of gas can be ejected at $\sim$ 100km/s perpendicular to the disk surrounds the star. When this gas interacts with the interstellar medium, it creates a shock. The shock can be responsible for Herbig-Haro(HH) objects (bright emission nebulae). The outbursts can be caused by increase rate of stellar accretion by a factor ≥ 100 for tens of years. This is seen in FU Orionis stars.

1.5 Observation of circumstellar disk

The detection of the excess emission at infrared wavelengths is an evidence of circumstellar material. The circumstellar material can extend out to ten or hundreds of AU from the star. 25-50% of the pre-main sequence stars e.g. T Tauri stars have this excess emission at infrared. The millimeter observations revealed many disk with masses between ~ 0.001 and 0.1 $M_{\odot}$.

HST has shown images of disk structures with radius extend out to 100 AU around young stars. The images of the disks around the stars HD141569 and HR4796A revealed inner holes. The disk of HD141569 has a radius of $\sim$ 750AU, and shows a dark area (a band) at the distance of approximately 300 AU which means that we do not have materials there. The material which has been there may have created a planet. The material may also have been pushed away by a planet's shepherding torque.

The disk of HR4796A has a clearly ring of dust at $\sim$40AU from the star. The ring is less than 17AU in size. All those rings can be explained by the existence of a planet. The Infrared Astronomical Satellite (IRAS) revealed the existence of cool clouds consist of solid particles. Those are found around the star Vega and some other main-sequence stars. The disks of these stars can extend out to a few hundred AU from the star, and they can have a lunar mass of material. The circumstellar disk around β Pictoris extends to 1500 AU. The inner part of βPic disk is warped. This can be produced by the gravitational pull of the nearby planet, or planets.

1.6 The Protoplanetary disk

Our Solar System is believed to be formed from the primitive solar nebula. A protoplanetary disk has a minimum mass of $0.02 M_{\odot}$, this value was derived under assumption that the elements abundances in the nebulae were solar.
To create a disk, solar nebulae must go through these stages; infall, internal evolution and clearing.

1.6.1 The infall stage

As mentioned in the last section, when cloud core gets very dense, its gravity becomes larger than the thermal,turbulent and magnetic forces, which cause the cloud to collapse. The time for this stage is similar to time of the free fall collapse of the core, and it is between $\sim 10^4$ and $\sim 10^5$ years. In the beginning, the gas and dust fall toward the core if they have a low angular momentum, and into the disk increase of high angular momentum. Because the centrifugal forces the dust never reaches the center.

The gas and dust fall against the system plane. On their way , they meet other material from other direction. As a consequence the motion which is perpendicular to the system plane

cancel. The energy produced is dissipated as heat in the disk, and especially in the inner part close to the protostar, where we have a deep potential well.

When the gas reaches a supersonic velocity on its way down, it slows abruptly when it passes through a shock front, as it accreted onto the disk. Here, the temperature becomes very high due to the shock. The typical temperature for protoplanetary disk is $\sim 1500K$ at 1AU, and $\sim 100K$ at 10AU. When the gravitational force toward the center becomes equal to the outward centripetal force, and in the same time the gravitational force toward the mid-plane becomes equal to the outward pressure gradient, the equilibrium state is reached.

1.6.2 The internal dynamical evolution of the disk

The disk has to get rid of its angular momentum, in order to acreate onto the star (angular momentum scales as $r^{1/2}$. The transport of angular momentum heat within the disk decides what structure the disk will take. The transport of angular momentum and mass can occur by three mechanism:
1.Magnetic torques; 2.Gravitational torques; 3.Viscous torques.

1.Magnetic torques: When the magnetic lines from the star go through the disk, then we get corotation. If the gas in the disk is ionized, the field lines couple the star to the disk. This is happened in the inner part of solar nebula, where the temperature is very high. The magnetic braking torque from the inner part of the disk slow down the spin rate of a rapidly rotating star.

In the inner part, the ionized gas couples to the stellar magnetic field, but it slowed by the collision with neutral gas, which orbits at the Keplerian rate. The magnetic interaction near the corotation point between the star and the disk pushes some of the disk's gas onto the star and expels the other gas in a rapid centrifugally driven bipolar outflow which carries with it a substantial amount of angular momentum.

2.gravitational torques: The instability of disk due to gravitation can make the transport of material within protoplanetary disk to occur very rapidly. The instabilities in a disk can produce a spiral density waves, which transport the mass and angular momentum on a dynamical timescale until the protoplanetary disk reach a stable structure. This process keeps the mass of the disk to be less or almost equal to the mass of the star. A one-armed spiral instability limits the disk mass to less than 1/3 of the star mass. In addition, a large protoplanet cleans a gap surrounding its orbits and gives tendency to density waves at resonant locations within the protoplanetary disk, which transport the angular momentum outward.

3.Viscous torques: All gas parcels orbit around the protostar at almost Keplerian orbits. The gas parcels close to the protostar evolve faster than those for away. The collisions between gas parcels in the outer part make the gas parcels to speed up and move outwards. In the same time, it slow down the gas parcels in the inner part of the disk, which make the gas parcels and matter to fall towards the center, which transport the angular momentum outwards, which in turn makes the disk to spread out.

2 Vega-type stars

The stars Vega and β Pic were considered standard stars. But after the discovery that they emit infrared excess of emitted radiation over the photo-spheric stellar flux, during the calibration of IRAS satellite in 1983 this idea changed.
The infrared excess is considered to be the thermal radiation of solid grain bigger than $1\mu m$ in size. This is larger than the typical grains founded in the interstellar medium. The grains which emit infrared has to be in their orbit around the star. The Vega-type stars definition requires that there is no mass loss. The Vega phenomenon that many normal main-sequence stars are surrounded by disk of dust. It has been established that approximately 1 in 5 main-sequence stars of type B, A, F and G do have circumstellar dust.

The Vega-type stars are believed to have planetary systems around them. Now, let us consider the prototype of the Vega-Excess phenomenon. There are four objects which considered prototype Vega system:
αLyr which is the Vega itself, it is a AOV star at 8.1 pc distance from us; αPsA which is an A3V star at 15 pc away from us; ϵEri, this is a K5V star at 3.3 pc distance from us; and β Pictoris which is an A5V star at 19 pc away from us, and it is the most studied star. β Pic has the largest absolute flux and absolute relative excess over the extrapolated photospheric contribution.

Smith & Terrile (1984) have for first time made an image of a disk-like structure in the scattered (visible/nearIR) light. The edge-on orientation and the sheer area of grains make β Pic to be visible.
According to a direct spectroscopy of Olofsson et al (2001), the disk is in the expected Keplerian rotation. The four objects have the spectral energy distribution close to a superposition of Planck curves with temperature range between 30K to 250K.

For α PsA the peak temperature is around $\approx$ 70K, and for αLyr is T $\approx$ 90K and for β Pic is T $\approx$ 110K. The different stellar luminosities make the black-body grain separation to be varied. For ϵEri it is 1 to 50 AU; αPsA it is 30 to 140 AU; αLyr it is 40 to 200AU and for β Pic from 15 to $>$ 400AU. All the temperatures are below 1500K (1500K it is the limit thermal evaporation of the silicate). A typical temperature of a disk is about 110K or less. This value of the temperature keeps the water ice unaffected by the thermal evaporation. There is a small fraction of solid grain in Vega-type stars which have temperature at about 200K. The solid grains make a clearing central (gap) in the disk. The density in the gap of β Pic between 10 and 40 AU is one magnitude less than the density in between 40 AU and outside. The gap may be caused by the dynamical effect of planets, or the ice evaporation boundary.

3 β Pic

The β Pic system are three components, the star , the dust and the sand surround the star, and the gas and plasma. The star is rotating rapidly and it is a mean sequence dwarf star of type A5V and $T_{eff} \approx$ 8200K. β Pic is near the zero-age main sequence and existed for T_{age} 20 – 40 Myr.

There is many evidence which strengths that β Pic is a young main-sequence star. The expected main-sequence life for β Pic is $\sim$ 1000Myr. The images taken on β Pic show the thin light-scattering disk seen nearly edge on. the two thin disk wings (NE and SW) stretch out to $>$ 2000AU from the star.

The result of HST observations show that the radial profile of the midplane surface brightness of the two disk wings is a power-low in term of x^{ν}. x is the projected distance from the star and ν is known to be different between $x \lesssim$ 100AU and $x \gtrsim$ 100 AU regions (Artymowicz */home/pawel/tex/other/heap/heap.ps*).

According to Artymowicz et al (1990), the exponent ν give a symmetric change between $\nu \sim$ -3 in the inner part, to $\nu \sim$ -4 in the outer part. This showed that there is an asymmetry with respect to the center. Both wings of the disk are equally bright at $x \lesssim$ 100AU, and the NE wing extends further from the star.

Modeling of the observed scattered light distribution has shown that the vertical optical thickness $\tau(r)$ falls with distance as $\tau(r) \sim r^{-1.7}$ in the interval $100 \lesssim r \lesssim 400$AU. The intrinsic vertical density profile of particles in the disk is best modeled by an exponential profile. At $x \gtrsim$ 120 AU the effective thickness of the disk grows linearly with x. The disk has a constant half-opening angle ($\sim 7^{\circ}$, Artymowicz et al 1989) or a slightly flaring profile (thickness$\sim r^{1.3}$). $\tau(r)$ is measured by the scattered light, and it is subject to substantial asymmetries in the disk. the first is wing-tilt, and caused by light scattering of particles in an inclined disk. This gives angular misalignment of wings by 1.3° , and it allows an estimation of the disk inclination (3°).

The second asymmetry is the butterfly asymmetry, and it is caused by the larger amount of dust on the SE side of the NE wing, and on the NE side of the SW wing. There is a warp-like asymmetry, which was found in the innermost regions. It was proposed that the inner disk part has a (3°) orbital inclination with respect to the outside disk (seen edge-on to within 1°).

3.1 The IR excess from the dust and sand

The dust around β Pic attributes to most stellar photo-spheric flux starting from 12μm IRAS bandpass and peaks in the 60 μm band . At far-IR and mm wavelengths, the dust radiates 10^2 more energy than the star. β Pic and Vega have only a ten fold far-IR exess, and that is because of a small amount of circumstellar dust. Their excess peaks at wavelengths corresponding to blackbody radiation with temperature T$\sim$ 100K.The excess of β Pic is wider than a single Planck curve and needs emission from black bodies with range temperatures T$<$ 50K to T $\sim$ 200. Vega-type stars have a large lack of hot grains (T $\gtrsim$ 200K) close to the star. In β Pic, those grains which have temperatures above the sublimation point for water ice are very rare (150K).

The size distribution dN $\sim s^{-3.5}ds$ of particles in collisionally evolved systems shows that the most mass is in the largest particles (s is the radius of the grain), and most area in the smallest. At least 0.13 M_E (M_E is the mass of the earth) of the dust and sand follows from the λ=0.8mm observations, and 0.5 M_E is found in the λ=1.3 mm observations. The ratio of wavelengths in millimeters and optical observation and the ratio of grain size studied is $\sim 10^3$, therefore the ratio of the derived masses must be $10^{3/2} \approx 30$, if we apply the $s^{-3.5}$ distribution

the optical/far-IR gives a minimum dust mass of about 1/300 M_E, which is consistent with the idea that β Pic dust is a part of a steady-state collisional cascade of planetesimals $\rightarrow$ rocks $\rightarrow$ pebbles $\rightarrow$ sand $\rightarrow$ dust, with the standard power-low size spectrum extending at least three decades in size from dust to sand.

The best observations which show the condition in the gap or clearing hole around the star is taken at $\lambda \approx 10\mu$m. If one compares between the thermal images and the scattered light images, one can see that the thermal flux increases more slower toward the center than the scattered flux. This can be related to the strong forward scattering of micron-size grains, as opposed to the isotropic thermal emission. The IR emission flux is not steeply rising close to the star, which means that the dust area is small near the star.

3.2 Silicates in the gap

The warm silicates at T $\sim$ 300K, which create 10 μm emission feature, were found spectroscopically by Telesco & Knacke (1991). If one considers the approximate temperature and location, the same particles can cause 10 μm emission feature and the thermal flux detected by IRAS. It requires $\sim 3 \times 10^{21} g (\sim 10^{-6}\ M_E)$ of silicates to produce the observed intensity of the line (this is 10^{-4} of the total dust mass in the disk).

If you consider Figure 1, you can see how the overlapping broad 9.6 μm and weaker 11.2 μm emission feature agree with Halley's comet dust feature, which peaking at 9.8μm. The interplanetary dust particles, or circumstellar disks do not make a better fit. The feature found in Halley is due to silicates. Different types of polycrystalline silicate mixtures fit the data. According to Bregman et al 1987, Campins & Ryan 1989, the mixture can be 56% of olivine, 36% of pyroxine, and 8% lattic-lager silicates.

According to Blanco et al.1991 the mixture consists of 95% amorphous olivine with cosmic abundances and 5% crystalline olivine. The strong line at 9-10 μm and the weak line at 11.2 μm in β Pic can be a result of amorphous or polycrystalline silicates (strong line), and crystalline olivine(weak line). The largest radii of silicates is between 1-2μm. The minerals olivine and pyroxene are believed to be candidates for the building of blocks of the solid bodies in our Solar System at present time, and they are anticipated in β Pic.

3.3 The spatial distribution of grains from combined visible and IR modeling

Using the power-law emissivities of mid-size grains, and assume that τ(r) is axisymmetric, which was done by Artymowicz et al (1989), gives an opportunity to measure the radial distribution of grains in the disk, and the central gap. Artymowicz et al.1989 tried with a one-component model of the disk (one type of grains).

For some range of grain emissivity models, the models place the half-density point of the disk at a temperature T=160K, and indicated that the density maximum coincides with T = 95-115K, allowing the main disk to contain stable water ice. The total cross-sectional area is $\sim 10^3$ AU^2, or in other words, it is a circle of 20AU radius (the area of the orbit of Uranus). For grains with size $\sim 4\mu$m and density of 1 g/cm^3, in this area will give the dust mass equal

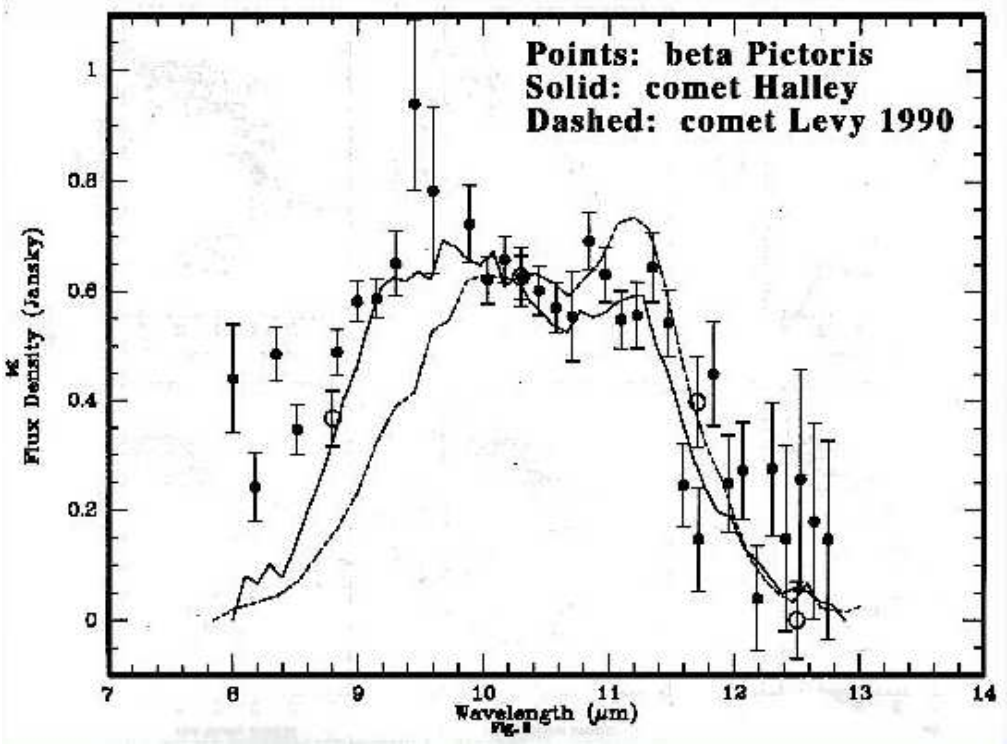

Figure 1: The broad 10 μm emission feature of warm β Pic silicates(points), compared with spectra of comet Halley(solid line) and comet Levy 1990 XX(dashed line), after subtraction of the cometary continum. The specyra were normalized at the 10.3-μm point.(Knacke and Fajardo-Acosta,1993.)

to 3×10^{25} g or 4×10^{-3} M_E.

Backman et al(1992) introduced a two-particle model of β disk, where the grains inside r = 80AU were allowed to have different properties than outside this radius. A piece-wise power-low spatial distribution of grains was used and measured the free parameters as the inner radius, normalization, and from the observations, the power indexes can be measured.

In order to measure the collisional and other timescales, one must quantify the total τ(r). One can introduce the τ(r), which is modeled after the preferred model solutions(e.g. the mid-size-grain model7 of Artymowicz et al(1989)) and agree with $\sim$ 30% with other available modeling, and then prove that the dust area decreases as r^p toward the star within $r \lesssim 40AU$, (with p=1 from the older, visible HST observations, and $p = 2$ is the 12μm map inversions and from the newer STIS/HST data (Artymowicz, 1999)).

Approximately the optical thickness can be given by the following formula:

$$\tau(r) = \frac{\sqrt{2}\tau_m}{\left[\left(\frac{r}{r_m}\right)^{-4} + \left(\frac{r}{r_m}\right)^{6}\right]^{1/2}} \tag{2}$$

where r_m = 50AU and it represents the radius where the density start to drop (from STIS

observations r_m= 120AU, I used also this value in my model). $\tau_m = \tau(r_m)$ is the optical thickness at r_m. If one want that the grains distribution to get correct percentage of the starlight, one needs to put $\tau_m \sim 10^{-2}$. In addition one must assume that 33% of the incoming stellar flux is absorbed by grains. If we want to compare between the dust distribution of β Pic to that of the Solar system-Zodiacal light(ZL), we see that ZL like β Pic disk has a nearly exponential vertical profile and scattering area proportional to exp[-4.2$(z/r)^{1.2}$] according to model done by Good et al (1986).

The ZL vertical profile has a scale height as z=0.3r, which is two or more times larger than for β Pic, i.e. ZL forms a thicker structure. The zodiacal dust has uniform radial distribution as $\tau \sim r^{-0.3}$ to$\tau \sim r^{-0.1}$, and this differs from the most grains in β Pic. The normalization of τ throughout the planetary system of our system is $\sim 10^{-7}$, much less than $\lesssim 10^{-4}$, a typical β Pic's value. All the differences we have are due to the different spatial density distribution of parent bodies, and not to basic nature of the phenomenon.

3.4 The properties of the grains

For the steady state size distribution we have N(s)$\propto$ $s^{-3.5}$ which derived from theoretical studies of inelastic collisions and fragmentation processes. This theoretical value is compared with the observations of asteroids and micro-meteoroids, and was adopted to β Pic system. The scattering properties of the grains is depended on the size of the grains. The color of the scattered light is the same as the color of the star within observational uncertainty between the range 0.4 and 0.9 μm, this indicates grains 1μm or larger in size.

Gradie et al. 1987 found also, a very red colors for the disk, V-I $\sim$ 0.6 magnitudes redder than the star. He also implied a grain size larger than 1μm. Measurements based on optical polarization give a size of $\sim$ 0.25μm.

Artymowicz (1988) has determined the ratio of radiation pressure forces to gravitational forces acting on small grains in the β Pic system. The stable minimum size is of order 1μm, and it may be larger if the grains are porous, or icy. There can be a size regime below which grains would couple inefficiently to β Pic radiation field and can be stable. The grains between 0.1 to 1μm can be a result of the rapid ejection from the system.

Artymowicz et al (1989) concluded that the β Pic disk has $9.10^{28} cm^2$ of optical scattering cross-section area in the region 100AU $< r <$ 500AU, and gives a value for albido of order 0.6 or 0.35 for the grains at r $>$ 100AU , this depends on the amount of the thermal radiation area attributed to same region. The albedo given here is very high comparing to small grains in different places on our Solar System such as zodaical dust grains.

3.5 Evidence for planetesimals

There is evidence for the existence of planetesimals from the variable absorption lines. By the time variable-absorption features was found that the solid bodies convert into hot plasma near the star. The absorption events can take from hours to many days.

The absorption is always reds-hefted by up to +300 km/s, but there is also blue-shifted events up to -60 km/s. The obseved ions feel a much stronger radiation pressure than gravity from the star, which mean that the rapidly infalling plasma is the material 'boiled off' of

infalling large solid bodies.

This calls Falling Evaporating Bodies (or FEB_s). The mass needed for evaporation per event is correspond to 1km planetesimals. The mass falls in a periodically 2-3 times per week. This and the large predominance of red-shifted features, suggest that the FEB_s belong to an orbital family with the mean orbit oriented in such a way that bodies approach the star when they are seen against it.

3.6 Do the planets exist?

We do not have indication of planet existing in β Pic, and the existing of planetesimals can not be used as indicators of planet existing. But there is a question about the reason which causes the observed disk thickness. The spread of orbital inclinations of dust and its parent bodies is of order 0.1 rad, this spread can explain the existence of $10^2 - 10^3$ moon-sized bodies in the disk. The requirement is that they have to be small to be able to avoid the concentration of matter around them. It is known that there are no giant planets outside r$\sim$ 100AU because their gravity will destroy the smooth power law of the disk brightness.The large bodies have opportunity to establish a vertical velocity spreading of small bodies around them. The order of this velocity is 0.1 times the Keplerian circular speed.

The escape velocity of largest bodies can be due to the lunar-class perturbers. What is the reason which make the FEBs (falling evaporating bodies) to reach the star?. Most scientists like to believe that there is at least one planet must be existing in order to explain FEBs.

This is because of the force of gravity of the planet is the only force that has the opportunity to rearrange the orbital distances and eccentricities of initially nearly circular orbits of planetesimals .

The photometric observations of β Pic show variations in the brightness of the star. It was an unusual brightening by 0.04 mag. within $\pm$ 10 days from November 10, 1981. Lecavelier et al (1995) assumes that the stellar activity can be responsible for those variations. They concluded that the variations are due to a giant planet passing in front of the stellar image. The brightening would then be followed by a planetary transit and again symmetric brightening. The area needed here is four times Jupiter's area and the distance is 0.08 AU from the star. Why would the brightening match the subsequent occultation, and the area of occultation is so large?. Why is the predicted brightening higher than theoretically based on the knowledge of dust density in the disk?. For comparison in our Solar System the Kuiper disk has a gap at $r \sim 40$ AU. The gap is caused by planetary perturbations of comets.

Roques et al (1994) and Lazzaro et al.(1994) made theoretical calculations, which show the effect of planet on a dust disk. This is allowed evolving under the gravitational perturbations of the planet and the Poynting-Robertson[1](PR) effect. The grains within size s = 1-20 μm affected by radiation pressure are trapped in the outer first-order mean motion resonances (1:2, 2:3, 3:4, etc), which has a damming effect on the inward PR drift and it may create a

[1]E.g., a particle in orbit around the Sun absorbs solar radiation and reradiates the energy isotropically in its own frame. The particle thereby preferentially radiates (and loses momentum) in the forward direction in the inertial frame of the Sun. This leads to a decrease in the particle's energy and angular momentum and causes dust in bound orbits to spiral sunward.

gap outside the planet's orbit.

The disk of β Pic is asymmetric, so why do we have asymmetry?.

Lazzaro et al 1994, studied the nonaxisymmetric, arc-shaped structures which caused by the perturbation from a slightly eccentric planet in a dust disk subject to the PR effect. The asymmetric structures rotate with angular velocities which are different from the angular velocity of the planet, but there is an amount dust, which corotating with the planet. But the results of those studies were too much interpreted and are wrong to make an application to explain the asymmetry of β Pic disk.

Kalas & Jewitt 1995 argued that the asymmetries in different places of the disk of β Pic need many planets in the disk.

There are conditions where the arc structures and asymmetries vanish; (Artymowicz 1994):
a) A wide range of initial eccentricities take place.
b) Collision between particles. The asymmetries take much dust area ($\sim 10^{28}\mathrm{cm}^2, \sim 10^{24}$), this is more than mass are given by collision of a pair of planetesimals or protoplanets. The fact is the idea of the interaction by dust-planet, which give indication of dust souces are shepherded by the planet.

But this is not responsible to more than $\gtrsim 25\%$ of asymmetries (Artymowicz 1994b). Scientists believed that the inner disk is warped due to the planets. The inclination we have in the inner disk may be explained the existence of planets. The planet orbits in inclined disk acts on the planetesimal and meteoroid in such a way as if the planet were rotating mutually-inclined rings, which behave as spinning tops: with other words they precess at a rate of which proportional to the perturbing mass.

If one Jupiter mass is at r=5.2 AU, then the inner region at $r \sim 40$ AU must be small oscillations around the planet's, more than around the disk's, plane of motion in just 15 Myr. But one can not be sure that the inclination is due to the planet and not to the planetesimal' orbits.

3.7 The physical processes in dust of β Pic

The radiation pressure has very important effect on the dust in β Pic disk. If the ratio of radiation pressure to gravity $\beta > 1$ (see equation (16) below) then the most neutral and ionized particles blow out from the star. This may conceivably lead to a slow migration of gas and solids because of a mismatch of their circular orbital velocities and the resultant weak gas drag. This is so especially because the small solid particles are affected by radiation pressure. During the formation epoch, the radiation pressure may have been instrumental in determining the Fe:Mg ratio of silicates under certain conditions. If, as in standard formation scenarios neglecting radiation pressure, the grains may have been differentiated into Mg-rich and metallic fractions, then radiation pressure could selectively have removed the most carbonaceous and ferritic grains into the interstellar medium.

When the ratio of radiation pressure to gravity $\beta > 1$, compact grains with radii $s \sim 1\mu$m blow out from the system (cf Artymowicz 1988). If the ratio of the gas to dust is $<< 1$, the blow-out process can not be stopped, because of the weak gas drag. All solid debris $< 1\mu$m escape from the system and especially if they are on hyperbolic trajectories. The fraction of

debris produced by collision escape from our system is observed as β-meteoroids (Zook & Berg 1975; orbitally stable particles are called α-meteoroids). This gives a good explanation for the color-neutral light scattering property of grains in the main disk.

3.8 Collision: creating and destroying the dust

When the grains are created, after a while they may be destroyed by collision. Substantial gas accretion does not occur. The kinematics of the disk stops grain buildup by collisions. The estimate of the speed can be made from the vertical motion speed $(z/r)v_K$, where $v_K \approx 38(r/AU)^{-1/2}$km/s is the Keplerian circular velocity, and $(z/r) \approx 0.1$ are certain to lead to net erosion, which starts at less than 0.1 km/s.

The geometrical cross section for grain–grain collision is $4\pi s^2$. A grain with e = 0 and inclination i = 7° will suffer a collision with a probability of τ(r) per one orbital period P. The effective optical thickness is $\approx \sqrt{1+(e/i)^2} \approx 3$ times larger in case of e = 0.33 and i = 0.12. The calculated collision time is given by

$$t_{coll} \simeq \frac{P}{12\tau} \tag{3}$$

where $P = 0.77(r/AU)^{3/2}$ year. $t_{coll} < t_{PR}$ for $r < r_m = 50AU$. This means that the Poyinting-Robertson effect is not important to β Pic disk. The disk destroys at the rate of

$$\frac{dM_{disk}}{dt} = 2\int \frac{dM}{t_{coll}} \tag{4}$$

where dM is the mass of the elements in the disk, which are considered as target, t_{coll} is the local collisional time, and the factor 2 is because of the two destructed grains.

Assume that we have N_β submicron debris, which are created from a collision between two grains at distance r_0 from the star. The debris accelerates to reach the final speed $(\beta - 0.5)v_K(r_0)$, which is larger than Keplerian speed v_K at the collision site. There will be a fraction of debris, which collide with the disk while they move out. They will collide at a speed, which is enough to fragment the largest disk particles and create even more debris.

Now, we can assume that N_β= const. that means, the flux of the debris depends on $\tau_\perp$ (the sign $\perp$ indicates the dust move perpendicular to the plane disk) and τ_{dust} of the dust. Then we have

$$\frac{dM_{disk}}{dt} \sim exp(N_\beta \tau_\perp) \tag{5}$$

or

$$\frac{dM_{disk}}{dt} \sim exp\left[N_\beta \tau_{dust}\left(\frac{z}{r}\right)^{-1}\right] \tag{6}$$

β Pic structure at present time is very dusty and the age is of order several dozen Myr, which is an indication of youth, the trace of the clearing period through which planetary systems pass after formation. There is an important issue that the ' internal sand-blasting' in β Pic disk is very active and need a huge amount of mass to be able to continue the erosion. The mass, which is needed around the same as the mass of solids in the Solar System.
Dust removal rate is scaling as

Now we have

$$\frac{dM_{disk}}{dt} \sim M_{dust}^2 \sim \tau_{dust}^2 \tag{7}$$

where M_{dust} is the total mass of the dust.

The disk of β Pic is not a low-mass Kuiper disk of an extra-solar disk, instead it is a substantial disk of planetesimals. We need more than $\sim 30 M_E$ Kuiper belts to be able to sustain a dust disk such as β Pic disk. In a steady state the total mass of planetesimal is equal to the total mass of dust times the square root of the the ratio of planetesimal to dust radius. The dust mass of order $M_{dust} = 10^{25.5} g$, of the grains, with size 4μm, and 1 km planetesimals, the planetesimal mass will be $\approx 125 M_z$.

As I mentioned before that the water ice is an important indication for planetesimals. But, there is no spectroscopic evidence for indication of icy dust.

The non-thermal photos-puttering destructs the ice rapidly through out the gap region and the whole disk. This can happened through two processes (Artymowicz 1994a);
1. the photo-desorption process: this is when the surface layer of H_2O molecules absorb stellar UV photons and get excited so the leading electrons eject.
2. The photolysis process: this is when the molecule eject into pieces.
Those processes are weak in our Solar system, because of the weak Solar UV flux between 1500$\mathring{A}$ and 1700$\mathring{A}$. The photos-puttering in β Pic makes the rate of size decrease to be given by $\dot{s} \approx -30(r/\mathrm{AU})^{-2} \mu$m/yr, this if we assume that one half of the grain surface is pure ice.

If the grains in β Pic have pure ice on their surface, the total photo-evaporation rate of the disk go up to 120 M_E in 4 Myr, and the unobserved dense water vapor cloud surround the star. There is another structure of icy dust composition. This icy structure causes the grain to break up into thousands of pieces in collision with another grain.

If the fragmentation strength of ice is more than the pure silicate part then during the collision the dust avalanches will be so strong that even a collision between two planetesimals in the inner disk is enough to make a destruction of a large part of the disk. But there is a inconsistency between the theory and observation. The theory predicts that the icy planetesimals collide and break into smaller ice-poor fragments, while the observations show ice-free dust.

4 The problem of gas mass in β Pic and the motivation of this work

Recently observations have given two different ideas about the β Pic disk. One is that the β Pic disk has very little gas: Lecavelier des Etangs et al(2001) made observations based on the far ultraviolet spectrum of β Pic, and they have not seen the H_2 absorption lines, which give them the opportunity to set a very low upper limit on the column density of H_2 : N(H_2) $\lesssim 10^{18}$ cm^{-3}, which gives M(H_2) $\sim 10^{-4} M_E$. Brandeker et al.(2003, unpublished) observed several gas species such as Na, Ca, Fe, Ti, etc., and derived the total gas mas assuming solar abundance ratios, M(gas)$\approx 0.02 M_E$.

The other idea is that β Pic has a large amount of molecular H (H_2): Thi et al (2001) made observations of emission lines from the lowest rotational transitions of molecular hydrogen (H_2), which give a mass of hydrogen $M(H_2) \approx 60 M_E$.

The purpose of this project is to make a dynamical modeling of the vertical structure of the dust in β Pic disk, and comparing the result with the observations, to try to resolve the gas problem.

4.1 Numerical model

In my numerical model, I was tracing the trajectories of a large number of particles representing dust grains created by collisions of larger, parent bodies (meteoroids). Since dust interacts with gas via gas drag and flattens the disk in time, my objective was to find how we can use the observed vertical distribution of dust to constrain the amount of gas.

Here are the main points about what I have modeled:

• I assumed a certain spatial distribution of dust sources along radius r and the vertical coordinate z.

• The vertical dust distribution I used was Gaussian with FWHM equal to $0.15r$.

• To follow the motion of partcles I used Euler method. I start with a single particle and put the time step $dt = 0.01 t_{dyn}$, where t_{dyn} is the dynamical time of the particle, and is given by the the following formula

$$t_{dyn} = \frac{1}{\sqrt{\frac{GM_b}{r^3}}} \tag{8}$$

where M_b is the mass of β Pic, r is the distance between the particle and the star and G is the gravitational constant. The number 0.01 is the value for which the particle keeps a circular orbit with sufficient accuracy.
I saved the history of the particle's position in each 30 time step. The maximum time is $t_{max} = 2\pi 6 t_{dyn}$ (6 orbital periods). Then I put 1000 to 10000 particles with grain size between $1\mu m$ and $800\mu m$ randomly distributed. I could not put larger number than this, because Matlab works very slowly.

• The velocities of grains are initially Keplerian, because parent bodies are assumed to have circular Keplerian orbits

• The stellar gravitation, radiation pressure and gas drag forces are acting on the dust grains.

• The radial distribution of the gas is a power-law , and outside the radius r_{out} the power law does not apply because the gas density is smoothly cut off. The vertical gas distribution is a Gaussian (see equation (33) below).

• From those information I modeled the vertical brightness, vertical number density distribution, radial brightness and x-y number density distribution.

• To compute brightness from dust density, I devided the latter by r^2, to account for the decreasing radiation flux illuminating the grains.

• In order to compare the vertical brightness with the observed profile I smoothed the profile by $0.15" \approx 3AU$, this is done because 'PSP'(Point Spread Function) of the instruments (HST) is at least 0.15".

4.2 The equation of motion

Let us go through the equation of motion (Taku Takeuchi and Pawel Artmowicz, 2001). For a dust grain carrying a mass m and has the position vector $\vec{r}$ the equation of motion is:

$$m\frac{d^2\vec{r}}{dt^2} = -\frac{GMm}{r^2}\hat{r} + F_{rad} + F_{PR} + F_g \tag{9}$$

r is the distance of the grain from the central star, $\hat{r}$ is the unit vector directed to the grain, M is the mass of the star and m is the mass of the grain.

The first term on the right side of equation (9) represents the gravitational force. The negative sign is because the force is directed toward the central star.

The second term represents the radiation pressure force, which is given by

$$F_{rad} = \beta\frac{GMm}{r^2}\hat{r} \tag{10}$$

β is the ratio of radiation pressure force to the gravity force.
We know that the radiation pressure force is approximately given by

$$F_{rad} \sim A_{grain}[flux\ of\ energy] \tag{11}$$

where $A_{grain}$is the cross section of the grain, and it is given by

$$A_{grain} = Q_{rad}\pi s_{grain}^2 \tag{12}$$

Q_{rad} is the radiation pressure coefficient averaged over the stellar spectrum.

$$flux\ of\ energy = \frac{L_*}{4\pi r^2} \tag{13}$$

The energy of photon is $h\nu$=E, and momentum=E/c= hν/c, So the radiation pressure force is given now by

$$F_{rad} = Q_{rad}\pi s_{grain}^2\frac{L_*}{4\pi r^2}\frac{1}{c} \tag{14}$$

β is given now by:

$$\beta = \left|\frac{F_{rad}}{F_{gravity}}\right| = \frac{Q_{rad}\pi s_{grain}^2\frac{L_*}{4\pi r^2}}{GM\frac{\frac{4\pi}{3}\pi s^3\rho_{grain}}{r^2}} = \frac{3}{16}\frac{Q_{rad}}{\pi GM}\frac{L_*}{sc\rho_{grain}} \tag{15}$$

If we substitute the values of all the constants in equation (15), we get:

$$\beta = Q_{rad}\left(\frac{2\mu m}{s}\right) \tag{16}$$

The value of β gives information about the orbit of grain.
The third term in equation (9) is Poynting Robertson force, and it is negligible because of the subsonic stopping parameter time in my calculations is very much less then unit (see below). The last term is the gas drag force F_g. If the grain has velocity υ, which differs from the velocity of the gas by $\triangle\upsilon = \upsilon - \upsilon_g$ and $|\triangle\upsilon| << \upsilon_T$ then the grain will feel a gas drag force, which is given by:

$$F_g = -\pi s^2 \rho_g \upsilon_T \triangle\upsilon \tag{17}$$

where ρ_g is the gas density, υ_T is the thermal velocity of the gas and it is given by

$$\upsilon_T = \frac{4}{3}\left(\frac{8kT}{\pi\mu_g m_H}\right)^{1/2} \tag{18}$$

k is Boltzmann's constant and m_H is the mass of the hydrogen atom,μ_g is the mean molecular weight ,T is the temperature, but in my calculation I used an approximate value for υ_T obtained from the assumption that the gas disk obeys:

$$\frac{\upsilon_T}{\upsilon_k(r)} = \frac{H}{r} \approx 0.15 \tag{19}$$

(following from a black-body tem.profile), H is the height. The gas drag force must be divided by the mass of the grain, the then we get:

$$F_g = -\frac{3}{4}\rho_g \upsilon_T \triangle\upsilon \frac{1}{s\rho_{grain}} \tag{20}$$

where ρ_{grain} as for water i.e. equal to 1 gcm^{-3}. The gas drag has a stopping time, which is defined as $t_s = m\upsilon/|F_g|$. We can write it as non-dimensional stopping time $t_s\Omega_K = T_s$, where $\Omega_K = (GM/r^3)^{1/2}$ is the Keplerian angular velocity. According to Takeuchi & Artymowicz (2001):

$$T_s = \frac{T_{ss}}{\sqrt{1 + \frac{(\triangle\upsilon)^2}{(\upsilon_T)^2}}} \tag{21}$$

where the square-root factor represents the supersonic correction. The subsonic stopping parameter time is given by:

$$T_{ss} = \frac{4\rho_g s \upsilon_K}{3\rho_{grain} r \upsilon_T} \tag{22}$$

if $T_{ss} = 1$, the grain will move slowly through the gas and couple to it in one dynamical time scale. If $T_{ss} \gg 1$, the grains are large and decouple from the gas disk. If $T_{ss} \ll 1$, in which the stopping time t_s is much smaller than the dynamical time scale Ω_K^{-1}, and the grains will move azimuthally at nearly the gas velocity. In case $T_{ss} < 1$, we have strongly coupled to gas disk. The velocity of the gas can be written as $\upsilon_g = \upsilon_K\sqrt{1-\eta}$, where η is the ratio of the pressure gradient force to the gravitational force. I used $\eta = 2.24 \times 10^{-2}$.

If $\beta = \eta$, the grains will have a steady circular orbit at a such distance r from the star, where $\beta = \eta$. Remember that in my calculation $T_{ss} \ll 1$, which means the PR drag force

is negligible. If $\beta > \eta$, the small grains in the gas disk circulate faster than the and move outward. In the case where $\beta < \eta$, the large grains rotate slower than the gas and start to move inward if PR drag is negligible, with other words the grains migrate inward if $\beta < \eta$ and outward if $\beta > \eta$. When $\beta > 1$, which means that the radiation pressure exceeds the gravity of the central star, the small grains in this case will blow away on a dynamical time scale, unless strongly braked by the friction against the gas.

If the grains have angular velocities, which are larger than of the gas, the grain will feel a head wind, which in turn make the grains to lose their angular momentum to the gas and start to move inward. If the dust grains experience strong radiation pressure, the orbital velocities of the grain will slow down and become slower than that of the gas.. This will make the grains to feel a back-wind, which gives the angular momentum to the grains, so that they start to move outward.

If we have a weakly coupled case ($T_s \gg 1$), and if $\beta \gg 1$, which means the radiation pressure force is very strong and dominated, the grains will accelerate their radial velocities, and their angular momentum will change a little, until they get large radial velocities, so that the radial gas drag becomes strong enough to balance with the radiation pressure. The size of dust grain depends on the grain' velocity.

4.3 The theoretical dust distribution

The number density distribution is given by the optical thickness $\tau_\perp(r)$, which is given by the following formula (Artymowicz 2002):

$$\tau_\perp = \frac{const}{\sqrt{X^{-4} + X^6}} \tag{23}$$

where $X = r_i/r_m$ (cf. section 3.3), the '$\perp$' is because the dust is perpendicular to the mid-plane. The shape of this distribution look as in Figure 2 (blue color). One can see that in the inner part ($< 120AU$) the profile has a shape of x^2 and for outer part ($r > 120AU$) has a shape of x^{-3}. The dust production rate is given by equation (7)

$$\frac{dM}{dt} \sim \tau_\perp^2 = \frac{const}{X^{-4} + X^6} \tag{24}$$

for $x < 120AU$ the profile has x^4-shape and for $x > 120AU$ it will have x^{-6}-shape.

4.4 The dust distribution

In order to calculate the vertical dust distribution, we have to calculate the number density n(p), where p is the parent body. The production rate of dust grain is equal to $\dot{N}_{prod}$, which in turn is approximately equal to the destruction rate of dust grain $\dot{N}_{dest}$ (parent bodies).

$$\dot{N}_{dest}(p) \sim -\frac{N(p)}{t_{dest}} \tag{25}$$

where N(p) is the number of particles and t_{dest} is the time scale of the particles' destruction by collision. The rate of destruction,

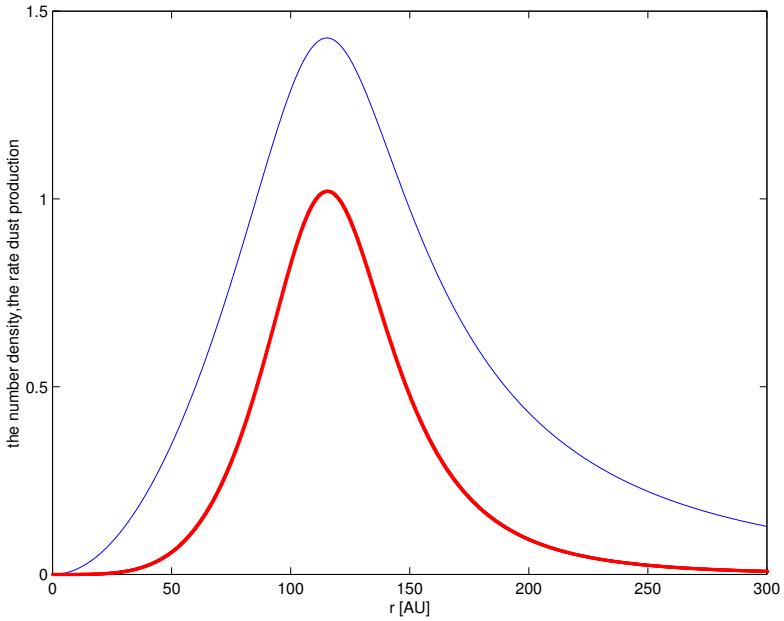

Figure 2: $r_m = 120AU$, r_i(1- 300AU), blue:the number density distribution, red: the dust production rate.

$$t_{dest}^{-1} \sim N(p) \sim n(p) \tag{26}$$

this gives

$$\dot{N} \sim -\frac{N(p)}{t_{dest}} \sim -N^2(p) \tag{27}$$

$$N(p) \sim n(p) \tag{28}$$

$$n(p) \sim \tau_\perp \tag{29}$$

where the optical thickness $\tau_\perp$ is given by equation (23). We have the destruction and production rates from (27) and (29)

$$\dot{N}_{prod} \sim \dot{N}(p) \sim \frac{const}{X^{-4} + X^6} \tag{30}$$

.

4.5 The observed vertical dust distribution

The observed vertical brightness profile is modeled according to the following formula (Artymowicz 1989)

$$I(z) = \frac{const}{w} exp\left(-\left(\frac{|z - z_c|}{w}\right)^p\right) \tag{31}$$

where w is the width of the profile in z-direction, z_c is the coordinate of the maximum dust density, p is power law index determining the shape of the vertical profile, $p = 0.7$ which corresponds to a central sharp core of density distribution observed by STIS/HST.

The observed vertical brightness is a radially-averaged of equation (31). My model are vertically distributed, but it is radially averaged.

4.6 Models and discussion

I used the power-law for gas density (Takeuchi and Artymowicz, 2001)

$$\rho_g = \rho_0 \left(\frac{r}{AU}\right)^q \frac{1}{2}\left(tanh\frac{r_{out}-r}{\triangle r_{out}}+1\right) \tag{32}$$

where r_{out} is the outer radius of the disk and it is equal to 300 AU,$\triangle r_{out}$= 12.1 AU, it is the characteristic edge-width of the disk. The above formula has only the radial gas distribution, but in model 6 ($M_g = 0.2M_E$) I put the vertical gas distribution, and for that the gas gas density becomes

$$\rho_g = \rho_0 \left(\frac{r}{AU}\right)^q \frac{1}{2}\left(tanh\frac{r_{out}-r}{\triangle r_{out}}+1\right) exp\left(-\frac{|z|^2}{w^2}\right) \tag{33}$$

where $w = 0.2r$, it is the half-width half-maximum, and ρ_0 is midplane density. Here it follows a table of the parameters I used in the models:

Table 1: All models

Models	$M_g(M_E)$	r_{out} [AU]	$\triangle r_{out}$ [AU]	q	number grains
1 (standard model)	10	300	12.1	-2.25	1000
2	0.001	–,,–	–,,–	–,,–	–,,–
3	0.1	–,,–	–,,–	–,,–	–,,–
4	1	–,,–	–,,–	–,,–	–,,–
5	100	–,,–	–,,–	–,,–	–,,–
6	0.2	–,,–	–,,–	–,,–	10000

where M_g is the gas mass. •Model 1: $M_g = 10M_E$
In Figure 3,the modeled profile of the brightness seems to have very high spike at z=0, and the wings drops as curvature near z=0. This due to the percentage of the height to the radius is 0.15. It can be also that I do not have enough particles to make the wings to be smoother.

The large peak at z=0 due to the large gas mass. The gas compresses the grains to mid-plane and creates a flattened disk.

Consider the vertical number density on Figure 5, you can see that there are two disks. The first one is thin and the most particles are compressed in mid-plane (due to the gas). The other disk is the extended disk which contains the very small or large particles, which move only up and down. The particles compressed to mid-plan are mid-size particles.

In Figure 4, the radial brightness has its maximum very close to the central star. The brightness drops very steeply between $r \sim$ 5AU and 40AU, then again decrease linearly until

$r \sim 120$AU and then it drops exponentially.

If we look at x-y distribution we can see a ring. This ring may due to the dust migration. The ring is weak, which means that the time I have chosen is short time for the dust to continue their migration. Consider also the trajectories of some fraction of dust while they are escaping from the system. They have spiral or hyperbolic trajectories. (see Figure 6).

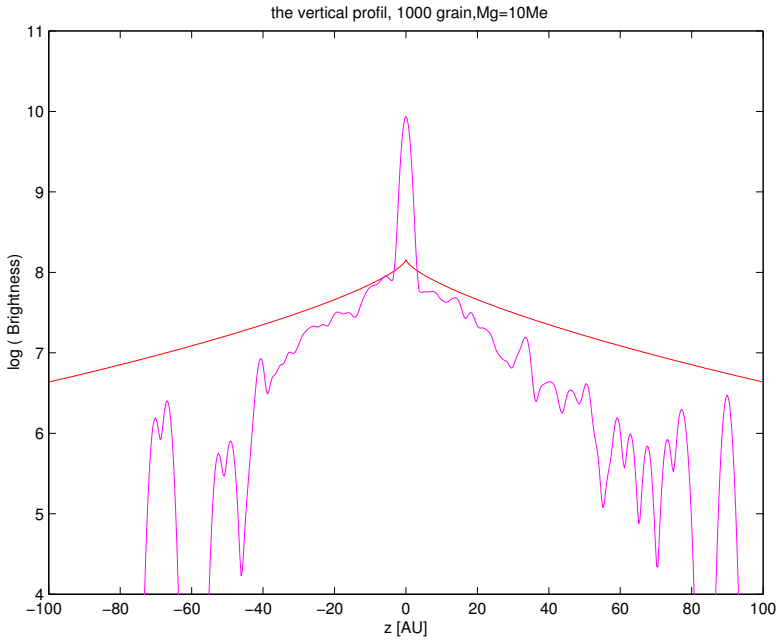

Figure 3: Model 1: $M_g = 10M_E$, the vertical brightness, the model has large spike, it does not fit the observed profile.

- Model 2: $M_g = 0.001M_E$

In Figure 7, the brightness profile does not have a peak, at z=0, but it drops almost exponentially. There is too little gas, so the grains do not experience a gas drag. The gravitation and radiation pressure forces are dominated. The grains have high velocities and they collide very often. If $\beta > 1$ the grains will blow out, and if $\beta < 1$ the grain will feel the gravitation force more and migrate inward toward the center.
On the vertical number density distribution in Figure 9, we see two disks. The most dust in the inner disk and close to the star, but here we do not see the flattened disk. The reason is the small amount of gas which can not compress the particles to the mid-plane. the extended disk have large or small particles, which move up and down.
In x-y distribution in Figure 10 , one sees the particles leave the system with straight trajectories. See also the radial brightness in Figure 8.

- Model 3: $M_g = 0.1M_E$

The vertical brightness profile in Figure 11 has a small peak at z=0. The wings are almost as in model 2, they are not symmetric. When we put more gas to the disk, the velocities of the grains decrease , this due to gas drag force,and therefore the grains are pushed by the gas to the mid-plane.
The radial brightness in Figure 12 is similar to the theoretical profile in Figure 2, (the red

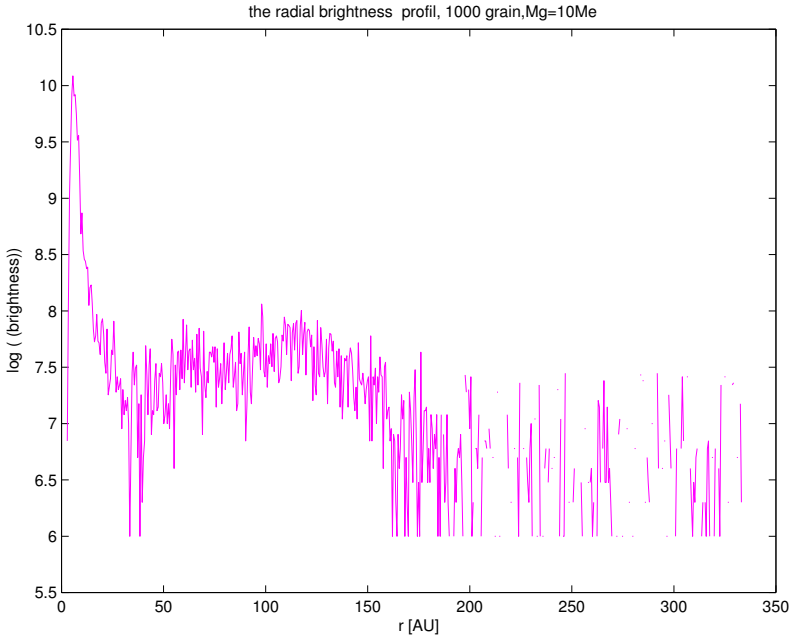

Figure 4: Model 1: $M_g = 10M_E$, the radial brightness.

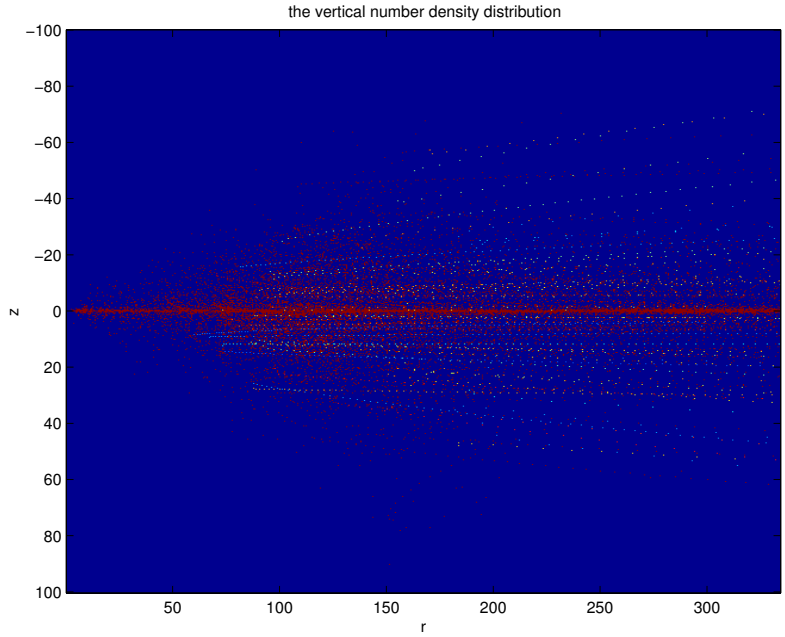

Figure 5: Model 1: $M_g = 10M_E$, z-r number density distribution [AU].

profile) for $r > 120$AU (cf. section 4.3).
In the vertical number density distribution in Figure 13, one can see how the dust compressed to form the thin disk. But as you see the thin disk is not so flattened in the outer part. This may be due the short integration time we have.
If you consider x-y distribution you can see how the dust are concentrated between 0-120AU, which due to the gas, one can also see how some particles escape from the system in parabola trajectories. (see Figure 14).

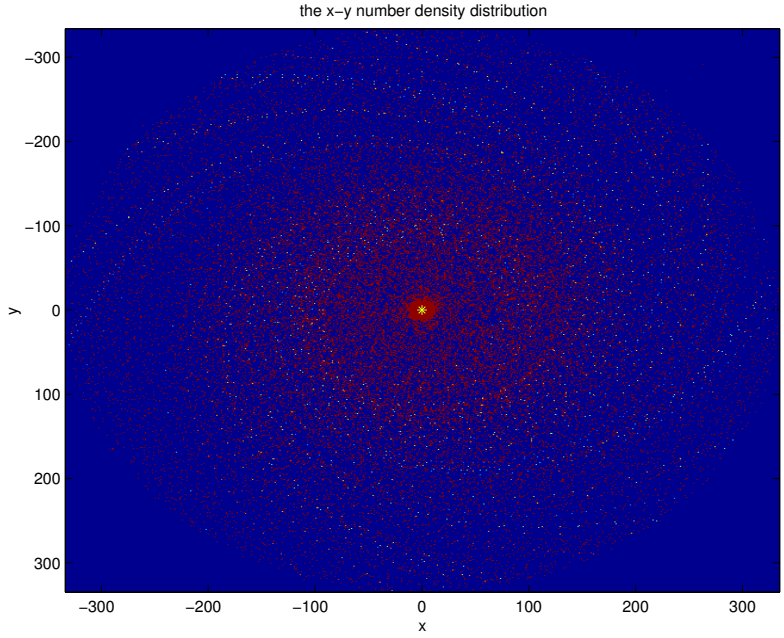

Figure 6: Model 1: $M_g = 10M_E$, x-y number density distribution [AU].

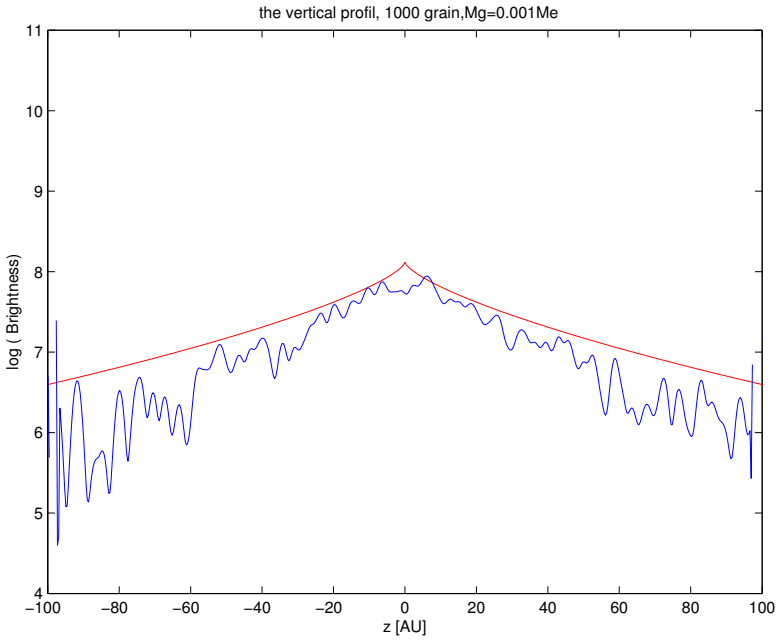

Figure 7: Model 2: $M_g = 0.001M_E$, the vertical brightness, the model has no peak, the wings approximately fit the observed profile.

- Model 4: $M_g = 1M_E$

The vertical brightness profile in Figure 15 has a large peak at z=0. The grains feel the gas drag force. The gas compresses the grains to mid-plane, and this why we get a large peak. Also the velocities of grains decrease due to amount of gas. The wings are curvature close to mid-plane and this due to the chosen height (0.15r). But otherwise the wings drops as the the

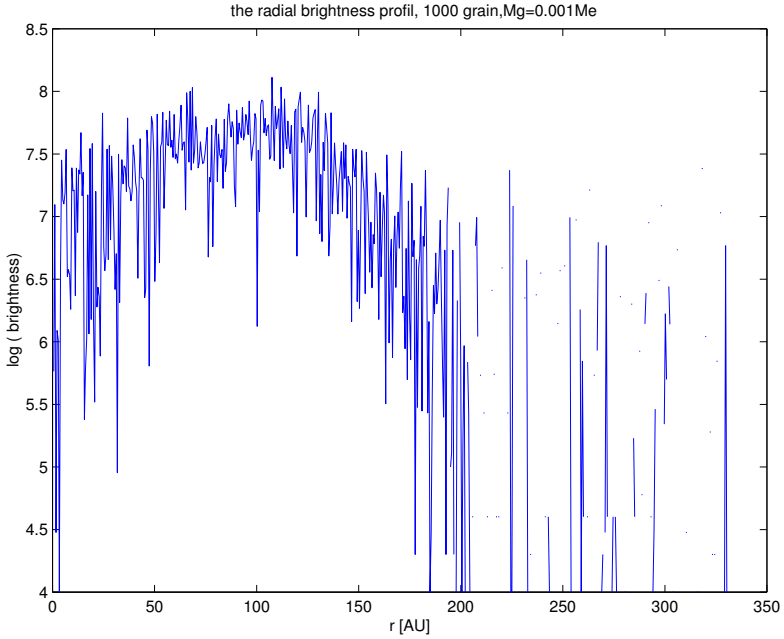

Figure 8: Model 2: $M_g = 0.001 M_E$, the radial brightness.

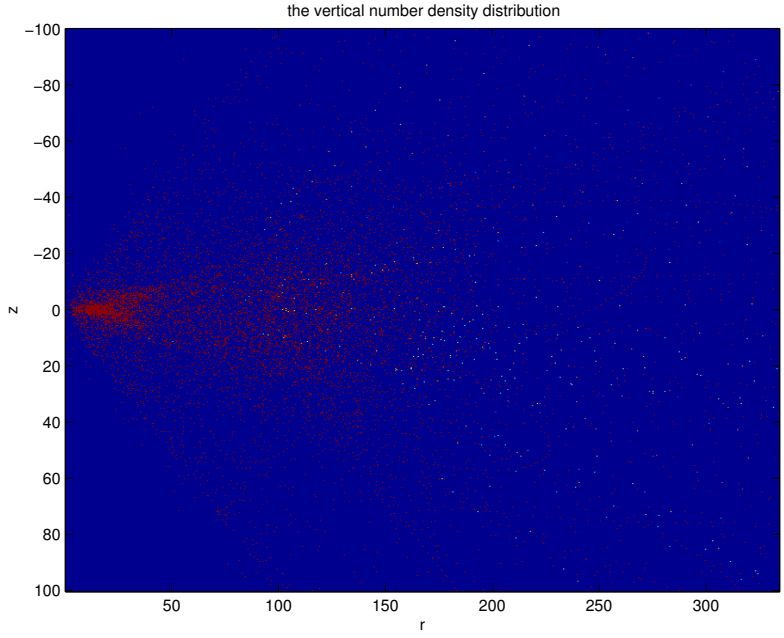

Figure 9: Model 2: $M_g = 0.001 M_E$, z-r number density distribution [AU].

wings of the theoretical profile, but the modeled profile is more noisy.
The radial dust distribution in Figure 16, shows a large amount dust very close to the star. Then at distance $r \sim 10$ AU the profile drops very steeply. At $r \sim 40$AU it starts to increase slowly and at 120AU it drops exponentially.
In vertical number density in Figure 17, we see that the flattened disk which contains the mid-size particles compressed by the gas is thiner than in the last model. In x-y distribution in Figure 18, one sees the dust falling toward the center star.This due to the grains which lose

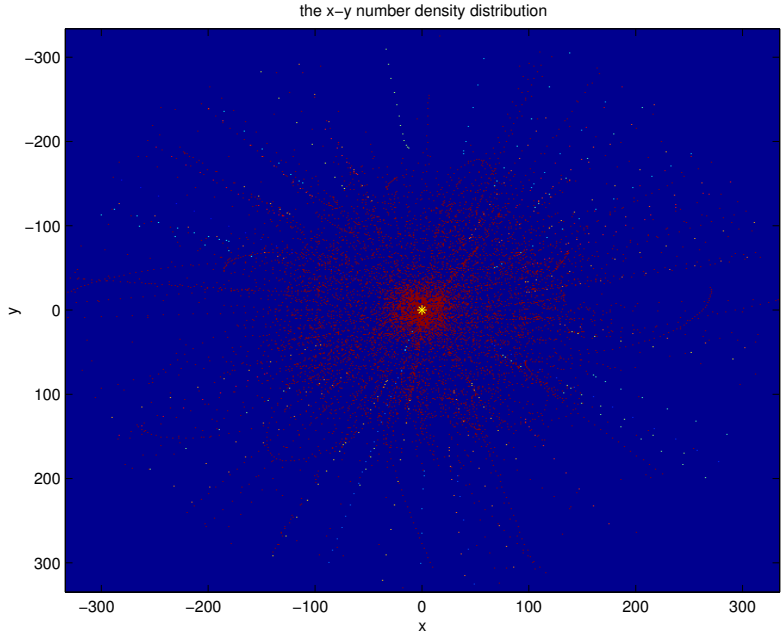

Figure 10: Model 2: $M_g = 0.001 M_E$, x-y number density distribution [AU].

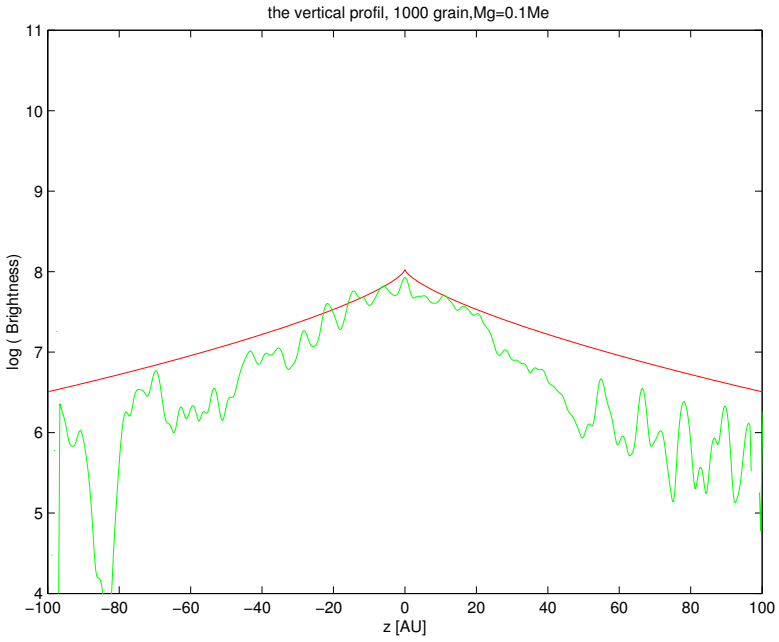

Figure 11: Model 3: $M_g = 0.1 M_E$, the vertical brightness, the model has a peak, but the wings are not symmetric.

their angular momentum to the gas and spiral toward the star.

Model 5: $M_g = 100 M_E$

In Figure 19 we the brightness profile is similar to that in model 4, but here the wings are destroyed. We have so much gas mass that the grains move very slowly, they are almost fixed, and they do not collide .

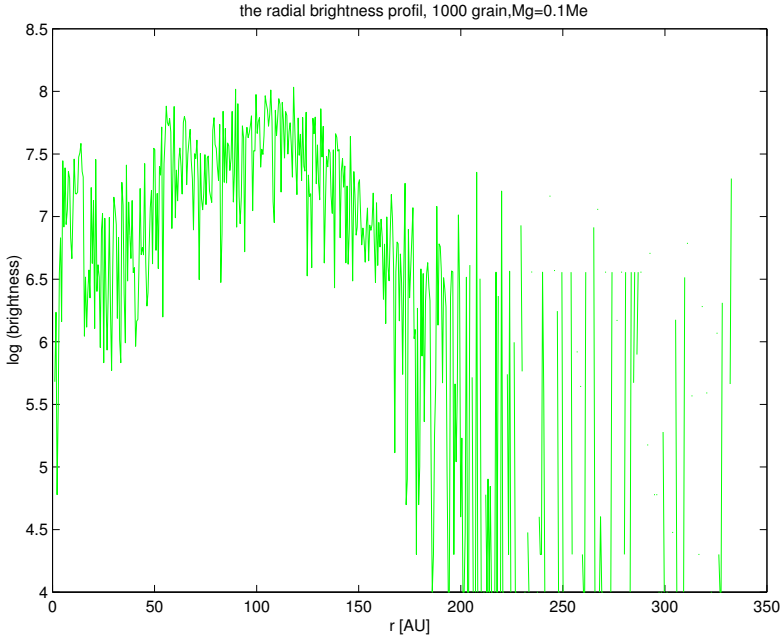

Figure 12: Model 3: $M_g = 0.1M_E$, the radial brightness.

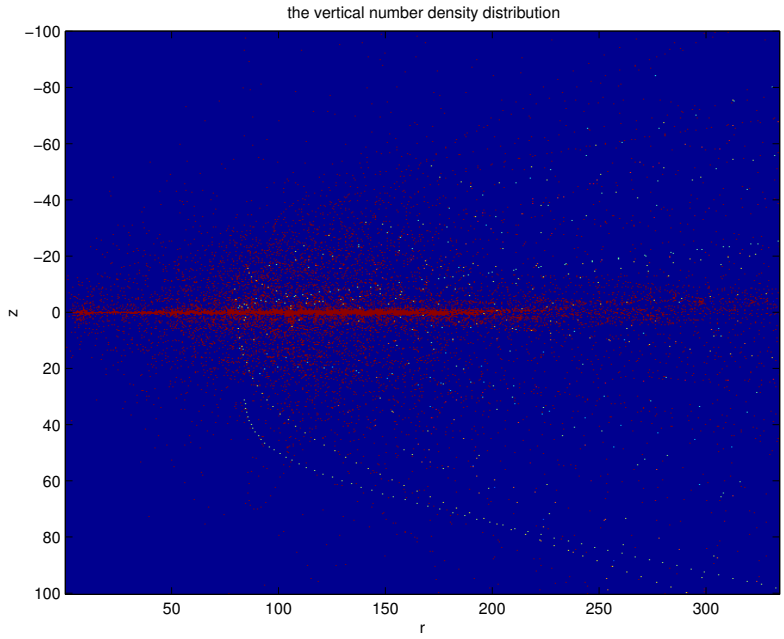

Figure 13: Model 3: $M_g = 0.1M_E$, z-r number density distribution [AU].

The vertical number density in Figure 21, shows how the particle's velocities are very low. One can see this in the x-y distribution in Figure 22. The disk is optically thick and so dense that most dust grains 'freeze' in the gas and are not able to migrate through it.

- Model 6: $M_g = 0.2M_E$

I choose this amount of gas because it looks from the profiles that a mass between 0.1 and 1 earth mass will give a better fit of the observed brightness. I put here 10 000 particles to be

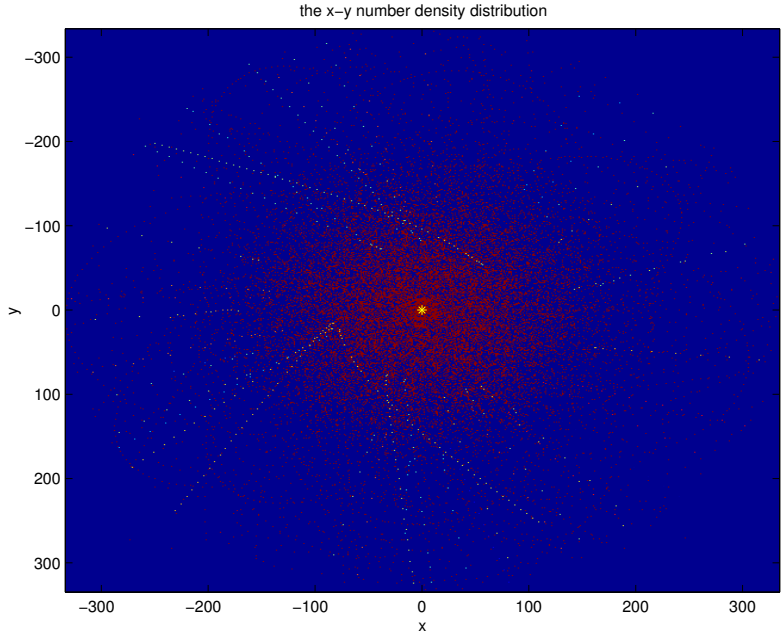

Figure 14: Model 3: $M_g = 0.1 M_E$, x-y number density distribution [AU].

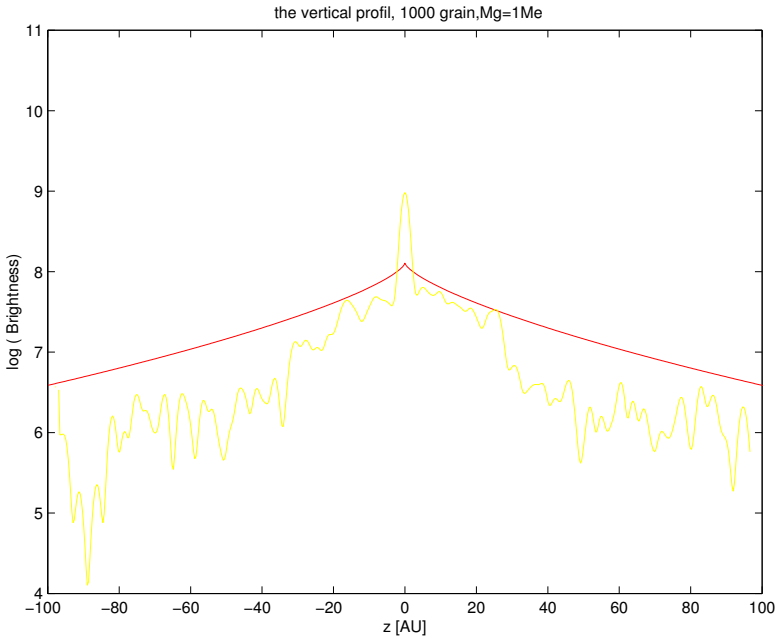

Figure 15: Model 4: $M_g = 1 M_E$, the vertical brightness, the model has a spike.

able to get smoother wings as the theoretical profile.

As you see the modeled vertical brightness approximately fits the observed profile. See Figure 23.

Consider also Figure 25 and Figure 26.

• take a look at figure(27). You can see very clearly that the only profile which fit the observed one, is model 6.

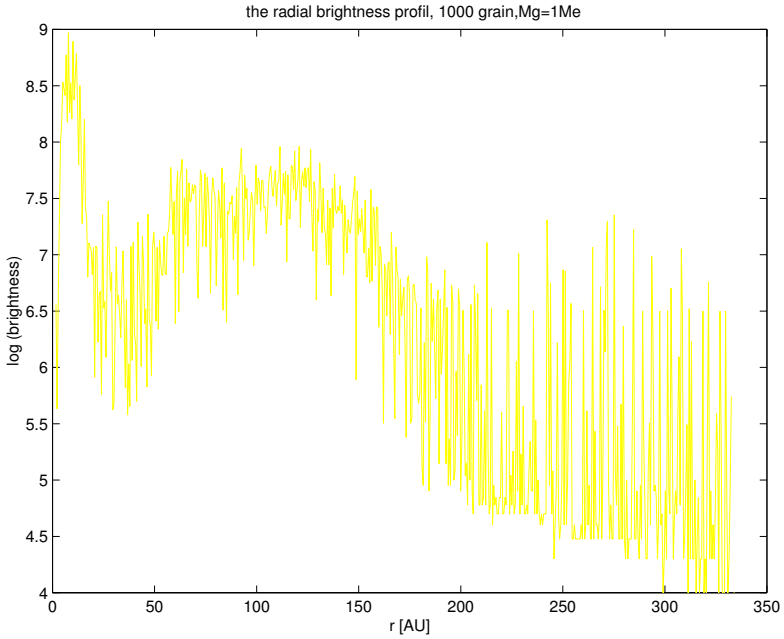

Figure 16: Model 4: $M_g = 1M_E$, the radial brightness.

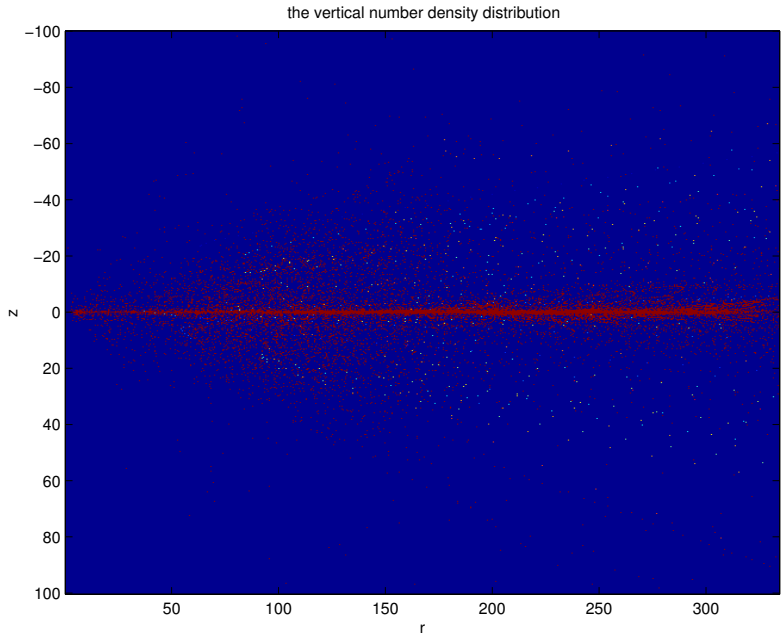

Figure 17: Model 4: $M_g = 1M_E$, z-r number density distribution [AU].

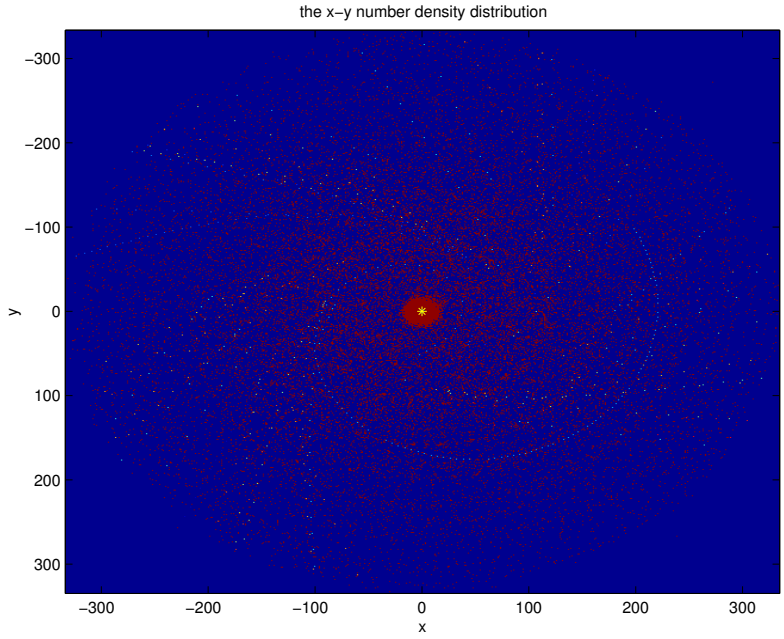

Figure 18: Model 4: $M_g = 1M_E$, x-y number density distribution [AU].

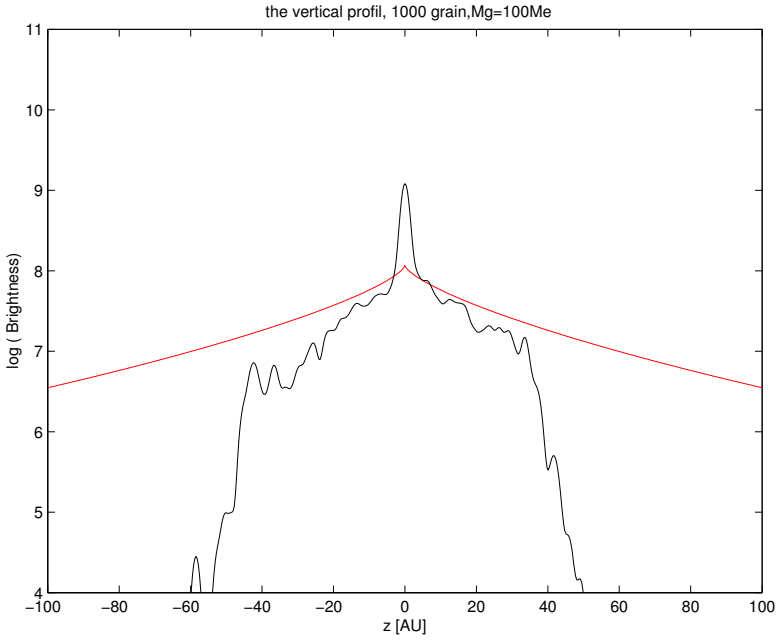

Figure 19: Model 5: $M_g = 100M_E$, the vertical brightness,the model has a spike and the wings are missing.

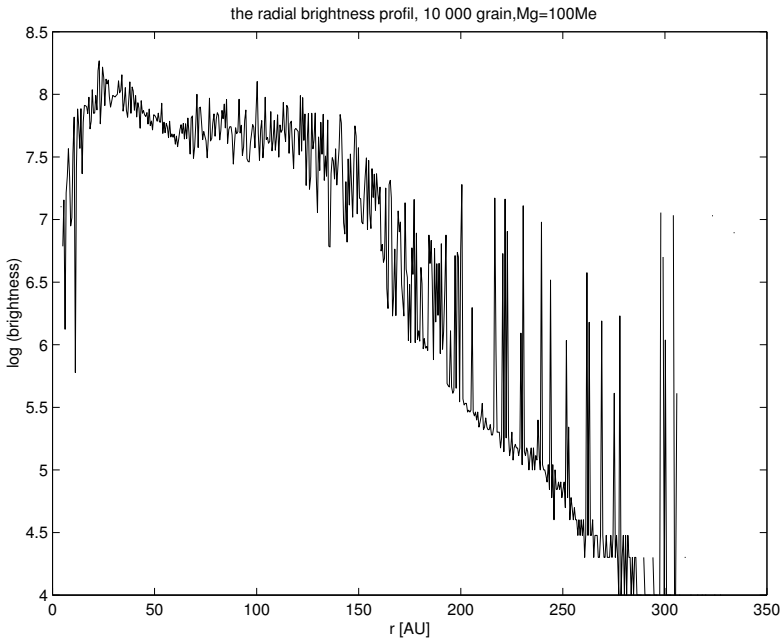

Figure 20: Model 5: $M_g = 100M_E$, the radial brightness.

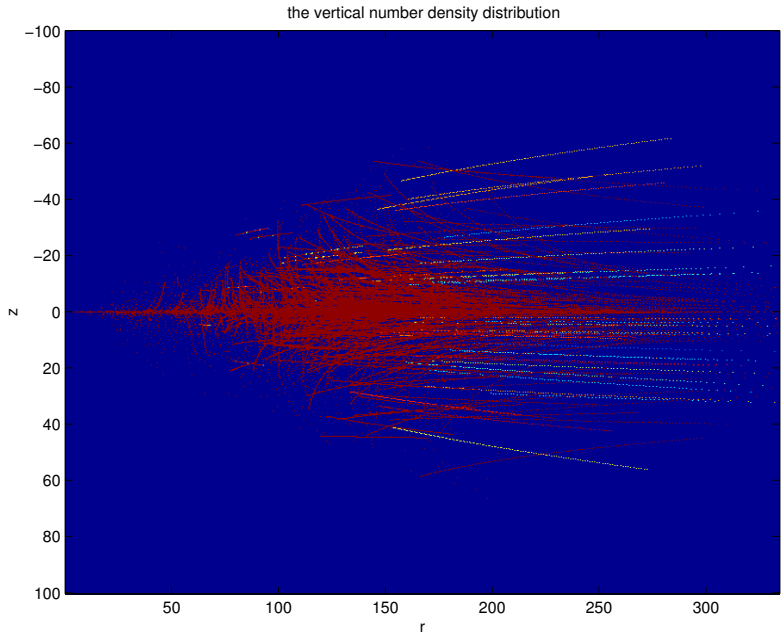

Figure 21: Model 5: $M_g = 100M_E$, z-r number density distribution [AU].

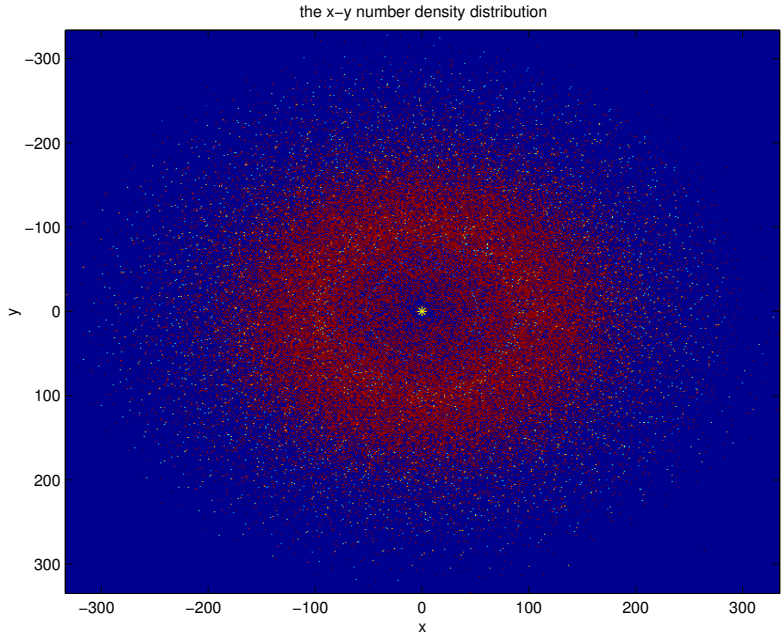

Figure 22: Model 5: $M_g = 100M_E$,x-y number density distribution [AU].

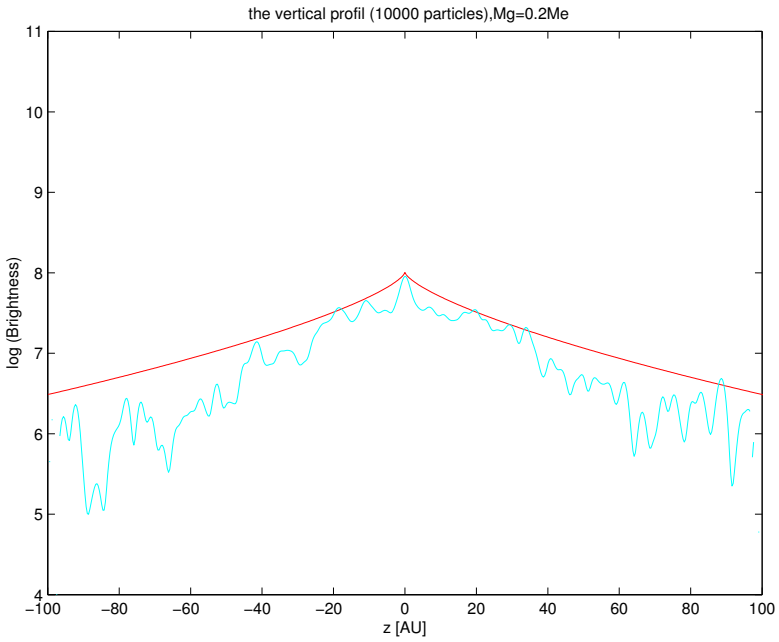

Figure 23: Model 6: $M_g = 0.2M_E$, the vertical brightness, the model approximately fit the observd profile.

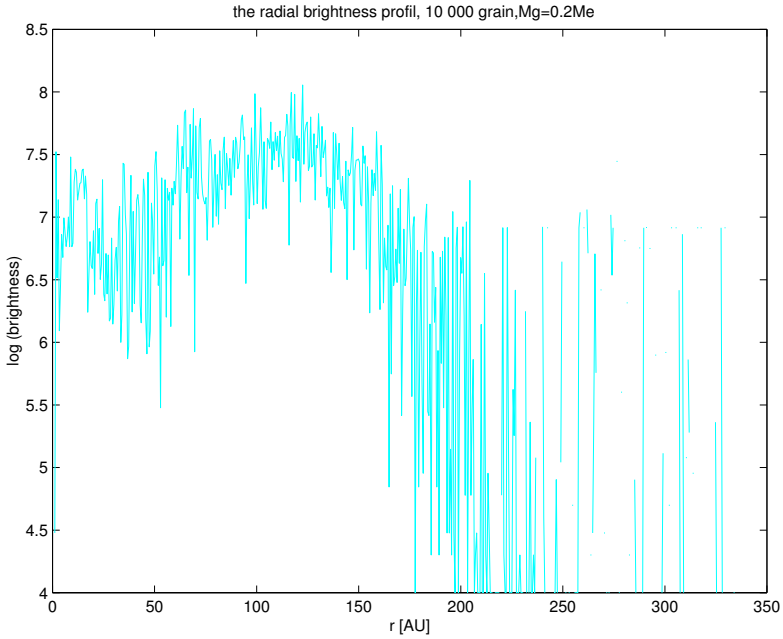

Figure 24: Model 6: $M_g = 0.2M_E$, the radial brightness.

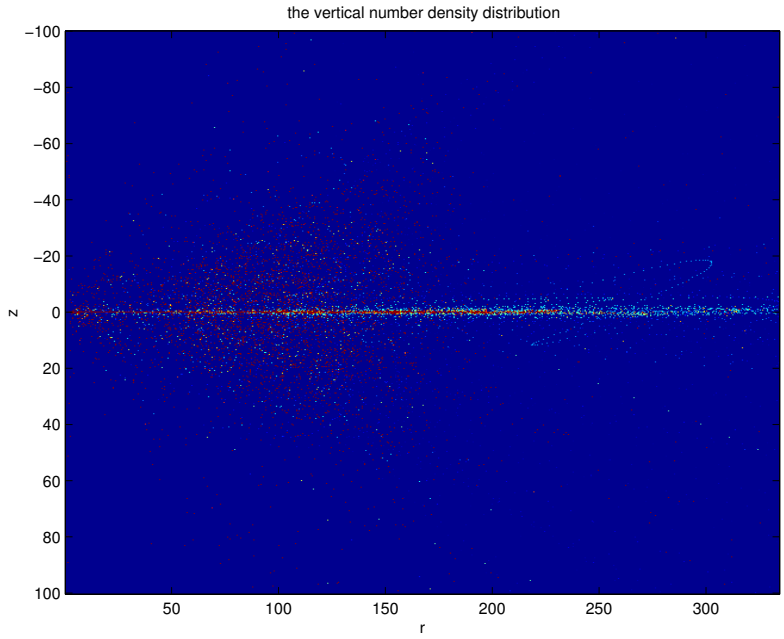

Figure 25: Model 6: $M_g = 0.2M_E$,z-r number density distribution [AU].

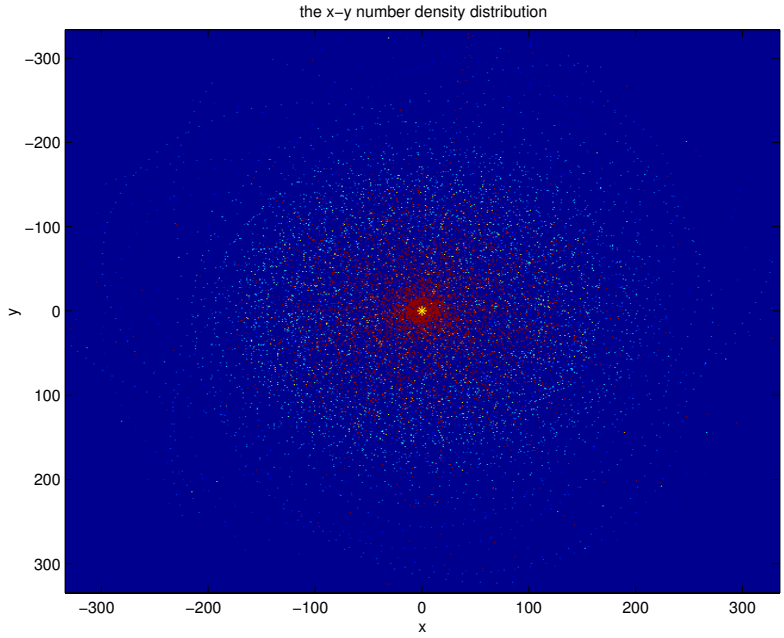

Figure 26: Model 6: $M_g = 0.2M_E$, x-y number density distribution [AU].

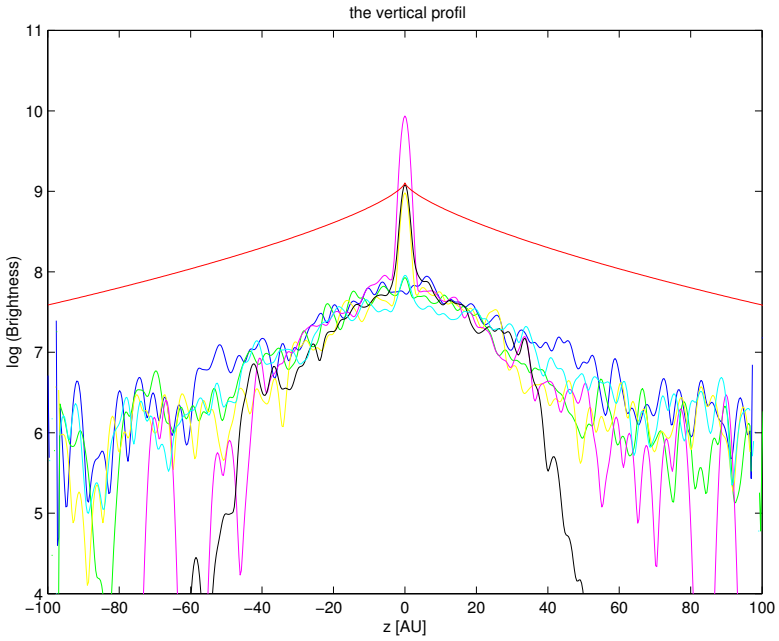

Figure 27: red: the observed brightness,blue (model 2):$M_g = 0.001M_E$, green (model 3):$M_g = 0.1M_E$, yellow (model 4): $M_g = 1M_E$, violet (model 1): $M_g = 10M_E$, black (model 5):$M_g = 100M_E$, light-blue (model 6): $M_g = 0.2M_E$. Only models 1, 4, and 5 have a central spike (thin disk).

5 Summary and Conclusion

• Vega-type stars differ from the other stars for their infrared excess, and the requirement that a disk of dust surrounded them, (cf. section 2).

• β Pic is a Vega-type star, and the disk has asymmetries close to the star, (cf. section 3).

• β Pic is a part of a steady-state collisional cascade of planetesimals $\rightarrow$ rocks $\rightarrow$ pebbles $\rightarrow$ dust.

The size distribution of particles in collisionaly evolved systems shows that the most mass is in the largest particles and the most area in the smallest, (cf. section 3.1).

• The emission feature at 10 μm is an indication of warm silicates existence at T $\sim$ 300K, (cf. section 3.2).

• The radial distribution of grains in β Pic disk, and the central gap is measured best by the power-law emissivities of mid-size grains, (cf. section 3.3).

• The scattering properties of the grains is depended of the size of the grains.

The red-shifted features of absorption lines caused by falling evaporating bodies belong to an orbital family with the mean orbit oriented in such a way that bodies approach the star when they are against it, (cf. section 3.5).

• There is an indication of planet(s) existence in β Pic, and the asymmetries and the inclination in the inner part of the disk can be explained by planets, (cf. section 3.6).

• The radiation pressure is one of the most important forces acting on the particles. It leads to particle migration, which is caused by a missmatch of their circular orbital velocities and resultant weak gas drag, (cf. section 3.7).

• The grains in the disk created and destroyed by the collision, and the buildup of grains is prevented by the kinematics of the disk. The disk decays at a rate proportional to the mass of elements (which act as a target) in the disk and the inverse collisional time. After collision the debris accelerate and reach final speed which is larger than the Keplerian speed at the collision site.

β Pic structure is very dusty, and the internal sand-blasting is very active. β Pic disk is not a low mass Kuiper disk of an extra-solar disk, instead it is a substantial disk of planetesimals, The observations of β Pic disk show ice-free dust, (cf. section 3.8).

• Some observations show that β Pic has small amount of gas mass and other show large amount of gas mass. The observations leads to a problem of gas mass.

• The gas problem can be resolved by a dynamical model of the vertical structure of the dust in β Pic disk, and comparing the result with the observations, (cf. sections 4–4.6).

• Model 1 ($M_g = 10M_E$): The modeled vertical brightness profile has a large spike (thin disk), and the wings are asymmetric. The modeled profile with such large gas mass does not fit the observed profile.

• Model 2 ($M_g = 0.001M_E$): The modeled vertical brightness has no peak, but the wings drop exponentially. The fattened disk does not appear in this model, this due to the little amount of gas. The modeled profile does not fit the observed profile.

• Model 3 ($M_g = 0.1M_E$): The vertical modeled brightness profile has a little peak at z=0. The wings drop exponentially, but they are little bit asymmetric. The modeled profile does not fit the vertical observed profile.

• Model 4 ($M_g = 1M_E$): The modeled vertical profile has a large spike at z=0, and the wings are asymmetric. The modeled profile does not fit the observed profile.

• Model 5 ($M_g = 100M_E$): The modeled vertical profile has a large spike at z=0, the wings are destroyed. The modeled profile does not fit the observed profile.

• Model 6 ($M_g = 0.2M_E$): The modeled vertical profile fits approximately the observed profile, the wings drop exponentially. The noise on the wings may be due to the small number of particles (10000 grains, for larger number Matlab is very slowly).

• There is only one model approximately fits the observed STIS/HST vertical profile, which is model 6.

• The observed mass of gas based on ultraviolet spectrum (Lecavelier des Etangs et al.2001) has $M(\mathrm{H_2}) \sim 10^{-4}M_E$. If we take in account the mass of the other molecules, then the mass of the gas will be higher and in such case model 6 will make sense. But we do not know how much other molecules are there.

• Brandeker (unpublished) observed several gases than hydrogen and got $\mathrm{M(gas)} \approx 0.02\mathrm{M}_E$ (assuming Solar composition). My results are not inconsistent with this estimate, especially that we do not know the actual abundances.

• The IR observations done by Thi et al (2001), and give $M(\mathrm{H_2}) \sim 60M_E$, if we take the other molecules then the total gas mass will be close to $\sim 100M_E$. This gas mass as we saw in my model does not fit the observed profile.

• β Pic disk according to the observation done by Lecavelier des Etangs et al.2001, and Brandeker A et al(unpublished), and my simulation is a gas-poor disk.

• If I would do this simulation again I would include the magnetic field. I would like to study the interaction of magnetic field with grains of different composition and size. I would attempt to model the radial distribution of dust in addition to the vertical distribution. I would allow such small interval of size in a given radius between r_1 and r_2 ($r_1 < r_2$). In the second model I would put other sizes between r_2 and r_3 and so on. In the end I would sum all models in one plot.

6 Appendix

Here it follows parts of the introduction which I thing are interesting, and you may read them if you are interesting.

6.1 The molecular cloud

The cloud will collapse because of own gravity if $|E_G| > 2E_k$. The cloud must have a minimum or critical mass to be able to avoid the collapse. This mass is the Jeans mass M_J, which is given by the formula:

$$M_J \approx \left(\frac{kT}{G\mu_a m_{amu}}\right)^{3/2} \frac{1}{\sqrt{\rho}} \tag{34}$$

If $M > M_J$,the cloud will collapse if the only support is the thermal pressure. According to above formula M_J will decrease if the density increase. If the density is low, the cloud will collapse into galaxy, and the opposite into clusters of stars or into a single star.
In order to form Jupiter-mass objects from gravitational collapse, in small cold (10K) cloud, the density must be larger than $\sim 10^{-11} g/cm^3$. This value of density is larger than density observed in interstellar clouds. The clouds and stars in our galaxy orbit faster than the pattern of spiral density waves rotation, therefore if a cloud passes through a spiral galaxy, the cloud will suffers compressing, which makes the collapse to be definitely real. This collapse known as (super)nova explosion. The collapse converts the gravitational potential into kinetic energy from the ejected shell of gas and dust. The cloud here is unstable and can be more unstable if the energy is lost by radiation . The collapse becomes faster due to the increased density.

6.2 The infall stage

The gas falls from the infinity to an orbits with radius equal to $R_\odot$ has half of the gravitational energy which convert to orbital kinetic energy and other half is converted to as heat i.e

$$\frac{GM_{protostar}}{2R_\odot} = \frac{v_c^2}{2} \tag{35}$$

per unit mass, where v_c is the circular velocity. If the protostar mass is equal to one solar mass, the circular velocity at 1AU will be 30 km/s, and the temperature is $\sim 7 * 10^4 K$ if the system is adiabatic.

If the gravity of protostar is dominates over the disk gravity , then the vertical pressure variation is given by

$$P_z = P_{z,0} e^{-\frac{z^2}{H_z^2}} \tag{36}$$

where H_z is the Gaussian scale height, and it increases due to the heliocentric distance as:

$$H_z = \sqrt{\frac{2kTr_\odot^2}{\mu_a m_{amu} GM_\odot}} \tag{37}$$

6.3 The internal dynamical evolution of the disk

1.Magnetic torques: The stellar magnetic field lines at larger distances are weak, and the ionized gas is small, both things make the transform of angular momentum at larger distance to be inhibited. The protoplanetary disk do not extend to the star surface. The lose of angular momentum makes the protostar to rotate less rapidly than break-up speed. The solid particles which expelled along with the gas are subjected to brief but intense heating by bright starlight.

2.Gravitational torques: This process was observed on small system as Saturn' rings. If the star have enough angular momentum, its lowest energy rotation state will be triaxial, which gives an asymmetric and rotating gravitational potential to the disk, and this can be caused by a protoplanet. This process will give need for resonances, and density waves, which in turn transport the angular momentum from the star to the disk. According to observations that $\sim M_{\odot}$ protostars rotate too slowly to become triaxial.

3.Viscous torques: The protostar disk evolves on a diffusion timescale according to following equation:

$$t_d = \frac{l^2}{v_\nu} \tag{38}$$

where l is the radial length scale which equal to the radius of the disk, and v_v is the velocity, depends on particle collision velocities and the local optical depth. The thermal motions of the gas produce a molecular viscosity, v_ν of order $v_\nu \sim l_{fp} c_s$, l_{fp} is the mean free path of the molecules and c_s is the speed of the sound.

The molecular viscosity is very small and it does not produce a significant viscous evolution over the lifetime of the protoplanetary disk. There is another process which gives angular momentum transffer. It is a turbulence which caused by the convection in nebula. The turbulent velocities are larger than the sound speed, and eddy sizes are larger than the scale height of the disk, this makes the turbulent viscosity of accretion disk is often parameterisized as:

$$\nu = \frac{2}{3} \alpha_v c_s H_z \tag{39}$$

where α_v is the viscosity parameter and it is less or comparable to 1. The α_v is calculated in an optically thick disk. The disk rate may depend on its optical depth perpendicular to the mid-plane. In the inner part of the protoplanetary disk is very hot for grains to condense out, and interstellar grains all have evaporated. The opacity sources in this part due to molecular transitions in, for example, H_2O and CO molecules and atomic hydrogen ionization processes.

The temperature in the outer part of the disk is below 2000K, and the opacity is due most to the micrometer-sized dust. The magnitude of the Rosseland mean opacity varies roughly as T^2, the radiation energy dissipated from the disk both faces, cools the disk. The convection perpendicular to the mid-plane of the disk, causes instability on the convection zone in the disk, this allows heat caused by convection to be transported from the hot mid-plane of the disk to the disk faces, and there the heat is radiated away into space.

The turbulence mixes the matter in the radial direction to a size of the largest convictive eddies. The temperature decreases with distance from the star and from the nebular mid-plane.

6.4 The chemistry in the disk

The chemical composition of the protoplanetary disk tells us a lot of information about planetesimal formation. The comets and chondritic meteorites are what left from planetesimal formation era of the Solar system's protoplanetary disk. the physical conditions, and the chemical compositions in a disk change over time when the matter in the disk accretes onto the central star, and when the planets form and when the disk scatters and leave a system as our Solar system.

The composition of the gas and dust in the interstellar medium and the chemical process later during the collapse decide what initial chemical state the disk will have. Different distances from star have different chemical composition. The abundances in the star tells us about the composition of the disk, because the star forms from the same matter as the disk, but the abundances do not tell us about the particular chemical compounds present. When the gas passes the shock front it is heated, but if there is matter added, the gas will be heated. The gas will be also cool if the dynamical evolution of the disk bring it close to the protostar.

If the temperature is larger than 2000K, one can calculate the chemical composition for nebular material. This large temperature is enough to evaporate and dissociate all incoming gas and dust, and the chemistry may assumed to be that of thermodynamic equilibrium, because of the rate of chemical reactions is faster than the cooling rate of the disk near the protostar. When the nebula reaches a cooling temperature, there the time of the chemical reaction is comparable to the cooling timescale the chemistry becomes complicated.

The freeze-out temperature is different for different elements. For example the ratio CO/CH_4 and N_2/NH_3 dependence very much on temperature and pressure, i.e they are very sensitive to temperature. CO is stable at T$\geq$ 700K. If carbon in the form CH_4, then it is stable at temperature less than 700K. Nitrogen is stable in form N_2 at temperature T$\geq$300K, and in form of NH_3 at lower temperature. That means, the disk at thermodynamic equilibrium will have the dominant elements CO and N_2 in the inner part, and the elements CH_4 and NH_3 in the outer part.

So, for example if the ices N_2 and CO exist anywhere in the outer nebula, this means that this part did not have enough time to chemically equilibrate. When the protoplanetary disk cools, the gas elements condense and undergo chemical reactions at different temperature. Oxides of aluminum , calcium and titanium (e.g., corundum Al_2O_3 and perovskite $CaTiO_3$) condense at temperature of $\sim 1700K$. The iron and nickel condense to form an alloy at temperature 1400K. Magnesium silicates appear at lower temperature, and as well forsterite($MgSiO_4$), and enstates($MgSiO_3$).

At temperature T$\lesssim 1200K$ plagioclase anorthite ($CaAl_2Si_2O_8$) appear and at T$\sim$1100K sodium and potassium felfspars($(N_{a,k})AlSi_8$). Aluminum can be included as feldspars only if it is contained in small grains, which may reach equilibrium with the surrounding gas. When the grain growth is rapid compared to the cooling, different minerals will form. When the chemical equilibrium is maintained chemical reactions in the gas and with the dust take place

as the temperature drops.

We have also an important reaction between iron and H_2S and forming troilite(FeS) at T $\sim$ 700K, the iron reaction with water and forming iron oxide(Fe+H_2O $\rightarrow$FeO+H_2) at T $\sim$ $500K$. A reaction between FeO and enstatite and forsterite form olivines and pyroxenes of intermediate iron content (e.g.,$(Mg,Fe)_2SiO_4$;$(Mg,Fe)SiO_3$). For $T < 500$, water is very important element.

The condensation is uncertain at low temperature, because there are other reactions occur at low temperature as ($CO+3H_2 \rightarrow CH_4 + H_2O$), and ($N_2+3H_2 \rightarrow 2NH_3$). The production of hydrated silicates are thermodynamically favored at low temperatures, but they have high activation energies. Those reactions take very long time to reach equilibrium state , longer than the nebula evolution allows, which make them to be Kinetically impossible.

At higher density, if equilibrium is reached, the water vapor reacts with olivines and pyroxones and forms hydrated silicates as serpentine $Mg_6Si_4O_{10}(OH)_8$, and hydroxides as brucite $Mg(OH)_2$. Pure water ice appears at $T < 200K$, and here ammonia and methane gas condense as hydrates and clathrates as NH_3H_2O and CH_46H_2O. At T $\lesssim$ 40K, CH_4 and Ar are in icy form. The 'non-equilibrium' elements CO and N_2 at T $\lesssim$ 60K with water ice form clathrates, and they may physically 'trapped' in water ice if it is cold enough. The species CO and N_2 condense into ice at T $\lesssim$ 25K.

The protoplanetary disk's outer cold regions have not reached an equilibrium, because of the time require to reach this state at low gas density such $\rho \sim g/cm^3$ and low temperature is longer than time requires for condensation and even it can be larger than the lifetime of the disk itself. This gives a consequence such as chemical reactions can be Kinetically impossible of reaching equilibrium. At the gravitational collapse $\sim$ 40% of the carbon in the interstellar medium is in the form of dust, and $\sim$ 10% is in polycyelic aromatic hydrocarbons, and at most of gas-phase C is in the form of CO molecules.

The element N_2 is in gaseous, but a fraction of nitrogen is in form of NH_3. It may not that N_2 and CO never convert to CH_4 and NH_3, and interstellar grains never evaporated. The present of NH_3 in cometary ices it may give evidence of interstellar origin. The ratio of D/H and $^{15}N/^{14}N$ in meteorites give evidence of origin in cold interstellar clouds. The ratio D/H is observed in comets, show that ices and other volatile compounds did not equilibrate with H_2 in the protoplanetary disk.

The abundances of CH_4:CO:C_2H_6 , H_2CO:CH_3OH and ubiquitous presence of S_2 and N_2 in comets also hint at compounds formed in cold interstellar clouds. That is mean that there is a fraction of the molecules in the icy grains from which the planetesimals formed originated in cold interstellar clouds and in the cold outer reaches of our solar nebula, and were incorporated as such in the forming bodies.

There is a disequilibrium chemistry in the evolving protoplanetary disk. The Galileo probe discovered increasing of volatile element C, N, S and noble gases Ar, Kr and Xe in Jupiter's atmosphere. Those elements have a wide range of condensation temperatures, which means that they were brought in by planetesimals which trapped within H_2O-ices at low temperatures, or it may be stable as solids. The iron in the disk are formed by cosmic rays, which

influence the evolution of molecules species. For example CO goes into CO_2, H_2CO and CH_4. N_2 goes into NH_3 and HCN. As the time runs, the abundances CO and N_2 decrease, and that depend on the ionization rate. Then the reactions which occur in equilibrium (Co goes to CH_4, and (N_2 goes to NH_3) are kinetically impossible. When the temperature becomes so low , that it can freeze out the gases, then these can be absorbed into grains. When the grains migrate toward the protostar, the ices melt again.

Another successful model explains the coexistence of ices as CH_4, CO and CO_2 in comets, and how the interstellar grains survived in the protoplanetary disk. It is clear that silicates and metal-rich condensates exist throughout the entire disk, but ices exist only in the outer part of the disk. The complex disequilibrium compound and both refractory and volatile grains of pre-Solar origin implies that the basic equilibrium condensation models are to simplistic. the planetary disk goes also through a clearing stage. Because presently there is no gas between planets, the gas must disappeared somewhere is one explanation for where the gas has gone, and it is that, the gas cleared when the pre-main sequence Sun went through its T Tauri phase of stellar evolution, approximately $10^6 - 10^7$ year after the protostar formed.

The gas may have cleared because of the Solar wind in T Tauri phase of stellar evolution, or by photo-evaporation from the surfaces of the disk induced by UV luminosity, or by UV photons from nearby massive stars. All four giant planets in our Solar System have approximatlythe same mass of rock and ice forming elements, but their H and He abundances vary by a factor of 100. This can be because the gas within the protoplanetary disk was dissipating as they were forming.

6.5 The properties of the grains

β Pic is classified as a shell star due to the presence of strong narrow circumstellar absorption features superimposed on the cores of some of the broad photo-spheric lines at ultraviolet wavelengths (Slettebak and Carpenter 1983; Kondo and Bruhweiler 1985; Lagrange et al.1987; Lagrange-Henri:et al 1988), and at visible wavelengths (Slettebak 1975; Hobbs et al. 1985; vidal-Madjar et al. 1986; Ferlet et al.1987; Hobbs et al. 1988).

In β Pic spectrum the shell absorption lines have complex multi-component structures in general can be decomposed into a strong stable component at the star's 21 km/s heliocentric radial velocity. There are an additional components, which are noticeable in the AlIII and MgII lines. Those lines are extremely variable in strength and velocity on time scales of days and month and they are always red-shifted with respect to the stable component.

The stable component correspond on a 'classical' A-F star shell. The meta-stable transitions of the CaII3d and FeII indicate that the radiation dilution must be $W > 10^{-5}$ in order that the rate of depopulation of the lower levels via spontaneous decay be negligible to radiative absorption (see, e.g. , Viotti 1976).

The radiative absorption indicates that the stable lines from ionized gas originate in material at $r < 1AU$. There is no correlation between the strength of far-infrared excess and the strength of spectroscopic A-F shell indicators (Hobbs 1986; Jaschek et al. 1986).

According to Jaschek et al. (1986), the frequency of far-infrared excess in A shell stars is

not anomalously high compared to ordinary A stars. The velocity dispersion parameters of b=1.8 km/s for NaI versus 3.7 km/s for Ca II k are evidence that the material producesing the neutral sodium absorption is connected to the grain disk because it seems to lie farther from the star than the ionized material in the shell.

The gas mass around β Pic is expected to be most in the outer component considering the radiative volumes and densities, and it would distinguish β Pic from 'classical' A-F shell stars. If one estimates the total gas mass around β Pic, one will get it to be less than $2M_E$, ($< 0.5\%$ of the mass in our planetary system) (Vidal-Madjar et al. 1986; Hobbs et al. 1988).

According to some results of a Model, there is indication that the gas near the star is roughly Solar-composition but the line strength imply that the region where the Na is located must be extremely depleted in Ca radiative to Na, this can be because the Ca is trapped in grains (Vidal-Madjar et al. 1986).

6.6 References

Artymowicz P, Beta Pictoris: An early Solar system?, annu.Rev.Earth Planet.Sci. 1997.25:175-219.

Artymowicz P, Beta Pictoris and other Solar systems, Space Sci.Rev.91: 63-80,1999.

Artymowicz P, Burrows C,Paresce F,The structure of β Pictoris circumstellar disk from combined IRAS and coronographic observations.Ap.J.337:494-513.

Artymowicz P, Paresce F,Burrows C,1990,The structure of β Pictoris disk and the properties of its particles. Adv. Space Res. 10(3):81-84.

Artymowicz P, Modeling and understanding the dust around β Pictoris,pp.47-65, 1994a.

Artymowicz P, Planetary hypothesis and the asymmetries in the β Pictoris disk,pp. 335-37,1994b.

Artymowicz P, Radiation pressure forces on particles in the β Pictoris system. Ap.J. Lett. 335:L79-82,1988.

Backman DE, Gillett FC,Witteborn FC, Infrared observations and thermal models of the β Pictoris dust disk, Ap.J., 385:670-97,1992.

Blanco A, Orfino V, Bussoletti E et al.,Laboratory spectra of amorphous and comet Halley IR spectrum,pp.125-28,1991.

Brandeker A, et al(2003, unpublished).

Bregman JD, Witteborn FC, Allamandola LJ et al., Airborne and groundbased spectrophotometry of comet P/Halley from 5-13 micrometers,Astron.Astrophys. 187:616-20, 1987.

Campins H, Ryan E, The identification of crystalline olvine incometary silicates, Ap.J., 341:1059-66,1989.

Hubertus Klahr and Doug Lin, Dust distribution in gas disks: A model for the ring around HR 4796A,ASP Conference Series, Vol.219,pp.375, 2000.

Kalas P, Jewitt D, Asymmetries in the β Pictoris dust disk,Ap.J. 110:794-804,1995.

Knacke RF, Fajardo-Acosta SB, Telesco CM et al., The silicates in the disk of β Pictoris, Ap.J. 418:440-50,1993.

Krivova NA, Krivov AV, Mann I, Size distribution of dust in the disk of β Pictoris,ASP Conference Series, Vol.219,pp.387,2000.

Lazzaro D, Sicardy B, Roques F. et al. ,Is there a planet around β Pictoris? Perturbations of a planet on a circumstellar dust disk.2. The analytical model.Icarus 108:59-80,1994.

Lecavelier des Etangs A,Vidal-Madjar A,Roberge A et al. Deficiency of molecular hydrogen in the disk of β Pictoris, nature 412. pp.706,2001.

Lecavelier des Etangs A. , Models of β Pictoris and disks around main-sequence stars,ASP Conference Series, Vol. 219,pp.308,2000.

Good JC, Hauser MG, Gauyier TN,IRAS,observations of the zodiacal backgrund,Adv.Space Res.6(7):83-86,1986.

Olofsson G, Liseau R, Brandeker A, Widespread atomic gas emission reveals the rotation of the β Pictoris, ApJL,Vol 563,Issue,pp.L77-L80, 2001.

Pierre-Olivier Lagage and Eric Pantin, The β Pictoris dust disk at 20 microns,ASP Conference Series, Vol.219,pp.393,2000.

Roques F, Scholl H, Sicardy B.et al.,Is there a planet around β Pictoris? Perturbations of a planet on a circumstellar dust disk.1.The numerical model.Icarus 108:37-58, 1994.

Smith BA,Terrile RJ, A circumstellar disk around β Pictoris.Science 226:1421-24,1984.

Taku Takeuchi and Pawel Artymowicz, Dust migration and morphology in optically thin circumstellar gas disks,Ap.J.557:990-1006,2001.

Telesco CM, knacke RF, Detection of silicates in the β Pictoris disk,Ap.J.Lett.372:L29-31,1991.

Thi WF, Blake GA, Van Dishoeck EF et al., Substantial reservoirs of molecular hydrogen in the debris disks around young stars, nature 409,pp.60, 2001.